MARMARA UNIVERSITY
INSTITUTE FOR GRADUATE STUDIES
IN PURE AND APPLIED SCIENCES

MODELING OF PH CONTROLLED ANAEROBIC FERMENTATION OF ULTRASOUND PRETREATED SEWAGE SLUDGE

ADNAN İNAN

MASTER THESIS

Department of Environmental Engineering

Thesis Supervisor
Prof. Dr. A. Evren TUĞTAŞ KARNABAT

Thesis Co-Supervisor
Asst. Prof. Hatice YEŞİL

ISTANBUL, 2025

MARMARA UNIVERSITY
INSTITUTE FOR GRADUATE STUDIES
IN PURE AND APPLIED SCIENCES

MODELING OF PH CONTROLLED ANAEROBIC FERMENTATION OF ULTRASOUND PRETREATED SEWAGE SLUDGE

ADNAN İNAN

MASTER THESIS

Department of Environmental Engineering

Thesis Supervisor
Prof. Dr. A. Evren TUĞTAŞ KARNABAT

Thesis Co-Supervisor
Asst. Prof. Hatice YEŞİL

ISTANBUL, 2025

ACKNOWLEDGEMENTS

I would like to express my deepest gratitude to my thesis advisor, Prof. Dr. A. Evren Tuğtaş, for her invaluable guidance, support, and expertise throughout this research. I am also sincerely grateful to my co-advisor, Asst. Prof. Hatice Yeşil, for her encouragement and insightful contributions, as well as for sharing her experimental data, which played a crucial role in the development of this model. A special thanks to Prof. Dr. Barış Çallı, who generously shared his knowledge and expertise throughout this thesis process. Additionally, I would like to extend my appreciation to İrem Güngördü, a fellow researcher in our study group, for her support and collaboration during this thesis.

I owe my heartfelt thanks to my beloved partner, Gülsuhan Kahraman, for her unwavering support, patience, and love, which made this process much more manageable. I am also deeply grateful to my mother, Rukiye Bingöl, my sister and brother-in-law, Yelda and Kerem Kurtay, and my dear nephew, Çınar Kurtay, for their constant encouragement and belief in me. Their presence has been a source of strength and motivation throughout this time.

I sincerely appreciate my uncle, Haydar Bingöl, a truly extraordinary person who has always encouraged me to see things from different perspectives. His unique way of thinking has been an inspiration throughout my academic development. I would also like to express my gratitude to my business partner, Utku Tunçer, whose vast knowledge and expertise have been invaluable. His deep understanding of biochemical processes, particularly those closely related to this project, as well as his insights into modeling, have significantly contributed to my research.

Lastly, I extend my sincere gratitude to the entire academic staff, administrative personnel, and blue-collar workers of Marmara University, whose efforts have contributed to the academic environment that made this research possible. I am truly grateful to everyone who has played a role in this journey.

February, 2025 **Adnan İNAN**

TABLE OF CONTENTS

ACKNOWLEDGEMENTS i
TABLE OF CONTENTS ii
ÖZET v
ABSTRACT vi
SYMBOLS vii
ABBREVIATIONS x
LIST OF FIGURES xi
LIST OF TABLES xii
1. INTRODUCTION 1
1.1. Sewage Sludge 1
1.1.1. Generation 1
1.1.2. Characteristics 3
1.1.3. Management 5
1.2. Anaerobic Digestion-Fermentation 7
1.2.1. Stages of anaerobic digestion 8
1.2.2. Influence of environmental factors on anaerobic digestion 10
1.2.2.1. Alkalinity and pH 10
1.2.2.2. Temperature 10
1.2.2.3. Organic loading rate (OLR) 11
1.2.2.4. Hydraulic retention time (HRT) and solid retention time (SRT) 11
1.2.3. Inhibition 12
1.3. Volatile Fatty Acid Generation using Anaerobic Fermentation 12
1.3.1. Importance of VFA recovery 13
1.4. Pretreatment Prior to Anaerobic Fermentation 14
1.5. Mathematical Modeling 16

1.5.1. Anaerobic Digestion Model No.1 (ADM1) 19
1.5.1.1. Dimensions of ADM1 19
1.5.1.2. Limitations of ADM1 24
1.5.1.3. Modifications of ADM1 for AD of pretreated sewage sludge and pH control in digesters 25
1.6. Objective of the Study 26
2. MATERIAL & METHOD 27
2.1. Experimental Data for Modeling 27
2.2. Experimental Data for Validation 27
2.3. Modeling of Anaerobic Fermentation of pH Controlled Ultrasound Pretreated Sewage Sludge through the Anaerobic Digestion Model No.1 28
2.3.1. Implementation of ADM1 28
2.3.1.1. Initial assumptions 29
2.3.1.2. Initial parameters 30
2.3.2. Parameter optimization - tunning 32
3. RESULTS AND DISCUSSION 34
3.1. Modeling via the Original Anaerobic Digestion Model No.1's Parameters 34
3.2. Model Results under Optimized Parameter Condition 35
3.2.1. pH - free ammonia nitrogen (FAN) 35
3.2.2. Disintegration and hydrolysis 37
3.2.2.1. Disintegration 37
3.2.2.2. Hydrolysis 39
3.2.3. Fermentation 44
3.3. Validation 48
4. CONCLUSIONS 50
REFERENCES 52

APPENDIX 1 66
APPENDIX 2 67
APPENDIX 3 68
CURRICULUM VITAE 82

ÖZET

ULTRASONİK ÖN ARITIM UYGULANMIŞ ATIK ÇAMURUN PH KONTROLLÜ ANAEROBİK FERMENTANSYONUNUN MODELLENMESİ

Bu çalışma, ultrasonikasyon ile ön işlem görmüş arıtma çamurunun pH kontrollü anaerobik fermantasyonunun, modifiye *"Anaerobic Digestion Model No.1"* (ADM1) ile matematiksel modellenmesini içermektedir. Günümüzde çamur ön arıtımlı ya da pH kontrollü anaerobik fermantasyonun modellenmesinde önemli ilerlemeler kaydedilmiş olsa da, bu iki faktörün sinerjik etkilerini gösteren bir çalışma bulunmamaktadır. Bu çalışmada, asidik, kontrol (nötr) ve alkali koşullarda, hem ön arıtılmış hem de arıtılmamış çamurla işletilen yarı sürekli anaerobik fermantörlerden elde edilen deneysel veriler, model optimizasyonu için kullanılmıştır. ADM1'de yapılan temel değişiklikler arasında; tüm pH koşulları için parçalanma ve hidroliz hız sabitlerinin, asidik koşul için uçucu yağ asitlerinin tüketim hızlarının ve alkali koşul için amino asitlerin stokiyometrik katsayılarının optimizasyonu yer almaktadır. Modifiye edilen ADM1, tüm pH koşulları için uçucu yağ asidi (VFA) konsantrasyonlarını doğru bir şekilde tahmin etmiştir. Asidik, kontrol ve alkali koşullar için toplam VFA konsantrasyonları model simülasyonunun son gününde sırasıyla 0.24, 0.032 ve 0.49 kg COD/m^3'ye ulaşarak, yine son günün deneysel toplam VFA konsantrasyon sonuçlarıyla (0.29, 0.032 ve 0.56 kg COD/m^3) yakından uyum sağlamıştır. Modifiye edilen model, model simülasyonları ile deneysel veriler arasındaki tutarlılığı incelemek amacıyla bağımsız deney sonuçlarıyla doğrulanmıştır. Bu şekilde model, farklı pH seviyelerindeki fermantasyon süreçlerinin belirgin dinamiklerini ortaya koyabilmiş ve alkali koşul için deneysel ve simülasyon sonuçları arasında güçlü bir korelasyon sağlamıştır. Bütün bu bulgular, ultrasonik ön arıtmadan geçmiş anaerobik fermantasyon sistemlerinin farklı pH koşullarında modellenmesinin etkinliğini vurgulamaktadır. Modifiye ADM1, benzer sistemlerin simülasyonu için sağlam bir temel sunmakta olup, ön arıtım teknikleri ile pH değişimlerinin sinerjik etkileri üzerine gelecekte yapılacak araştırmalara yeni ufuklar açmaktadır.

Anahtar kelimeler: ADM1, pH kontrolü, arıtma çamuru, ultrasonikasyon, VFA üretimi

ABSTRACT

MODELING OF PH CONTROLLED ANAEROBIC FERMENTATION OF ULTRASOUND PRETREATED SEWAGE SLUDGE

This study presents the mathematical modeling of pH controlled anaerobic fermentation of ultrasound pretreated sewage sludge using a modified Anaerobic Digestion Model No.1 (ADM1). While significant progress has been made in modeling both sludge pretreatment and pH controlled anaerobic fermentation, no study has yet demonstrated the synergistic effects of these two factors. In this study, experimental data from semi-continuous anaerobic fermenters operated under acidic, control (neutral), and alkaline conditions, with both pretreated and non-pretreated sludge, were used for model optimization. Main modifications of ADM1 included adjustments of disintegration and hydrolysis rate constants for all pH conditions, utilization rates of volatile fatty acids under acidic condition, and the stoichiometric coefficients of amino acids under alkaline condition. The modified ADM1 accurately predicted volatile fatty acid (VFA) concentrations for all pH conditions. The total VFA concentrations in model simulations for acidic, control, and alkaline conditions reached 0.24, 0.032, and 0.49 kg COD/m^3 on the final day, respectively, closely aligning with the experimental total VFA results (0.29, 0.032, and 0.56 kg COD/m^3). The modified model was validated with independent experimental results to examine the consistency between the experimental data and the model simulations. Thus, the model depicted the distinct dynamics of fermentation processes at varying pH levels, achieving a strong correlation between experimental and simulation results under alkaline conditions. These findings highlight the effectiveness of modeling anaerobic fermentation systems pretreated with ultrasonication under different pH conditions. The modified ADM1 provides a solid foundation for simulating comparable systems, opening new avenues for future research on the combined effects of pretreatment techniques and pH variations.

Keywords: ADM1, pH control, sewage sludge, ultrasonication, VFA production

SYMBOLS

Bar : Pressure unit Bar

Cu : Copper

Cd : Cadmium

$CaCO_3$: Calcium carbonate

CH_4 : Methane

CO_2 : Carbon dioxide

C_i : Concentration of component i

C_x : Concentration of microorganisms

d : Day

day^{-1} : Per day

DM/year : Dry matter per year

$f_{x,y}$: Fraction of component x inside of component y

g/cm^3 : Gram per cubic centimeter

g TS/L.d : Gram total solids per liter day

$HCO3^-$: Bicarbonate

H_2 : Hydrogen

H_2S : Hydrogen Sulfide

I : Inhibition

J : Joule

K : Kelvin

K_h : Rate constant

K_m : Maximum specific uptake rate constant

K_s : Half-saturation constant

K_2O : Potassium oxide

kg COD/m^3 : Kilogram chemical oxygen demand per cubic meter

kg COD/m^3·d: Kilogram chemical oxygen demand per cubic meter day

kg VS/m^3.d : Kilogram volatile solids per cubic meter day

kmole C/m^3 : Kilo mole carbon per cubic meter

kmole N/m^3 : Kilo mole nitrogen per cubic meter

kW/L : Kilowatt per liter

kHz : Kilohertz

L : Liter

MJ/kg VSS : Megajoule per kilogram volatile suspended solids

mg/L : Milligram per liter

mg NH_3-N/L : Milligram ammonia per liter

mL : Milliliter

Mt : Metric Tone

N : Nitrogen

P : Phosphorus

Pb : Lead

PHAs : Polyhydroxyalkanoates

pH : Minus logarithm of hydrogen ion concentration

pH_{LL} : Lover pH limit

pH_{UL} : Upper pH limit

$pH_{UL,aa}$: Upper pH limit for acidogenic and acetogenic microorganisms

P_2O_5 : Phosphorus pentoxide

q_{in} : Flow rate in

q_{gas} : Flow rate of gas

q_{out} : Flor rate out

S : Substrate

S_i : Concentration of soluble component i

$S_{liq,i}$: Concentration of soluble component i inside of liqueur

$S_{in,i}$: Concentration of soluble component i in

T_{resX} : Residence time of solid components above HRT in the reactor

t : Time

UV : Ultraviolet

V_{gas} : Gas volume of reactor

V_{liq} : Volume of liqueur inside of reactor

X : Biomass

X_i : Concentration of particulate component i

$X_{in,i}$: Concentration of particulate component i in

$X_{liq,i}$: Concentration of particulate component i inside of liqueur

Y : Yield coefficient

Zn : Zinc

% : Percent

^oC : Celsius degree

ρ : Process rate

ρ_j : Process rate of j

ρ_{gasT} : Gas transfer rate

$v_{i,j}$: Biochemical rate coefficients of component *i*

ABBREVIATIONS

AD : Anaerobic digestion

ADM1 : Anaerobic Digestion Model No.1

COD : Chemical oxygen demand

EU : European Union

EPA : U.S. Environmental Protection Agency

FAN : Free ammonia nitrogen

HRT : Hydraulic retention time

IWA : International Water Association

LCFA : Long chain fatty acid

LCFAs : Long chain fatty acids

OLR : Organic loading rate

OLRs : Organic loading rates

PFRP : Process to further reduce pathogens

PSRP : Process to significantly reduce pathogens

SRT : Solid retention time

TS : Total solids

TR : Türkiye

USA : United States of America

VFA : Volatile fatty acid

VFAs : Volatile fatty acids

VS : Volatile solids

VSS : Volatile suspended solids

WWTP : Wastewater treatment plant

WWTPs : Wastewater treatment plants

LIST OF FIGURES

Figure 1.1. Sludge generation flow diagram of WWTP 1

Figure 1.2. Urban sewage sludge disposal in 2022 6

Figure 1.3. Generalized sludge processing flow diagram..... 7

Figure 1.4. Anaerobic fermentation-digestion pathway of organic material 8

Figure 1.5. Distribution of composite 21

Figure 1.6. Reactions in anaerobic fermentation in reactor 22

Figure 1.7. Dynamic environment of ADM1 23

Figure 3.1. Total VFA concentration simulations of original ADM1, without any modification..... 34

Figure 3.2. pH levels in the acidic, control (neutral), and alkaline reactors 35

Figure 3.3. Free ammonia nitrogen concentration at pH 10 (a), pH 5, and pH 7 (b) 36

Figure 3.4. Model behavior during disintegration of composite material 38

Figure 3.5. Fate of carbohydrate (a), and sugar (b) modeled via modified ADM1 40

Figure 3.6. Fate of protein (a), and amino acid (b) modeled via modified ADM1..... 42

Figure 3.7. Fate of lipid (a), and long chain fatty acid (LCFA) (b) modeled via modified ADM1 43

Figure 3.8. Fate of total VFAs modeled via modified ADM1 45

Figure 3.9. Fate of acetic acid (a), propionic acid (b), butyric acid (c), and valeric acid (d) modeled via modified ADM1 47

Figure 3.10. Total VFA concentration comparison between experiment and model (a), and R^2 value of model (b)..... 48

Appendix 2-Figure 1. Mass balance analysis for modified model 67

LIST OF TABLES

Table 1.1. Sewage sludge generation 2

Table 1.2. Primary and waste activated sludge characteristic 4

Table 1.3. Units 19

Table 1.4. Liquid phase components 20

Table 2.1. Initial assumptions 29

Table 2.2. Initial variables of experiment modeled 30

Table 2.3. Modified stoichiometric parameter values of amino acid in the modified ADM1 31

Table 2.4. Optimized parameters in the modified ADM1 32

Appendix 1-Table 1. Percentage calculation of VFAs derived from amino acid 66

Appendix 1-Table 2. Hydrogen included partition percentages of amino acid 66

1. INTRODUCTION

1.1. Sewage Sludge

Sewage sludge is an ultimate byproduct of wastewater treatment processes, consisting of the solid residues removed during the treatment of domestic, industrial, and even stormwater runoff (Demirbas et al., 2017; Tyagi & Lo, 2013). It generally consists of up to 98% water and is commonly observed as a semisolid slurry. The solids content in the sludge, however, can range from 0.12% to 12%, based on the specific unit processes and operations utilized in sludge management facilities (Ghangrekar, 2022). The proper management and utilization of sewage sludge are critical for sustainable wastewater treatment, as it not only contributes to environmental protection but also offers potential pathways for resource recovery (Lee et al., 2014). Over the decades, sewage sludge has transitioned from being viewed solely as a waste product to being considered a valued source for energy and nutrient recovery, especially considering circular economy initiatives (Wichelns et al., 2015).

1.1.1. Generation

Wastewater treatment plants (WWTPs) produce sewage sludge as a result of their operation, removing organic and inorganic solids from wastewater. These processes occur in multiple stages such as primary, and secondary treatment in WWTPs (Figure 1.1) (Wichelns et al., 2015).

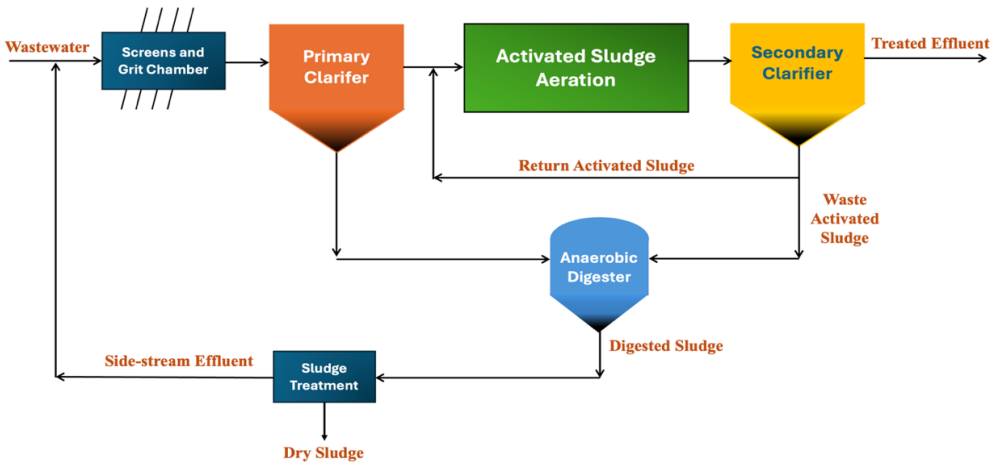

Figure 1.1. Sludge generation flow diagram of WWTP - Adopted (Sancho et al., 2019; Yeşil, 2021)

Primary treatment involves the removal of settleable solids during sedimentation, which generates primary sludge (Ghangrekar, 2022) (Figure 1.1). Secondary treatment focuses on biological processes to degrade organic matter, producing secondary (or activated) sludge as microorganisms multiply and form biomass (Tchobanoglous et al., 2014) (Figure 1.1).

The quantity and composition of sewage sludge depends on several factors, including the volume and composition of influent wastewater, treatment technologies employed, operational efficiencies, and seasonal variations (Ghangrekar, 2022). With increasing urbanization, industrial activities, and population growth, global sludge generation is on the rise, resulting in mounting pressure on existing sludge treatment and disposal systems (Table 1.1).

Table 1.1. Sewage sludge generation

Country	Sewage Sludge, mt DM/year	Year	Reference
USA	6.5 - 13.8	2004-2017	(Seiple et al., 2017; Wichelns et al., 2015)
EU	13.5	2016	(Kiselev et al., 2019)
China	6.25	2013	(Kiselev et al., 2019)
Germany	1.7	2021	(Eurostat, 2024)
France	1.1	2022	(Eurostat, 2024)
Türkiye	0.35	2022	(Eurostat, 2024)
Greece	0.1	2021	(Eurostat, 2024)
United Kingdom	1.1	2012	(Eurostat, 2024)
Spain	1.2	2018	(Eurostat, 2024)

Considering the quantity of sewage sludge generation, the United States (USA) and the European Union (EU) together produce more sewage sludge than the total produced by other countries combined (Table 1.1). Besides, Türkiye (TR) has approximately generated

0.35 mt DM/year in 2022 according to data by Eurostat (2024)(Table 1.1). Table 1.1 also indicates that sewage sludge generation and development status of countries can be related with each other. Nowadays, in urban areas where the human-being mostly live, sludge production is expected to increase further, necessitating the development of advanced management strategies to handle this growth sustainably (Ghangrekar, 2022).

1.1.2. Characteristics

The sewage sludge composition is variable and affected by wastewater characteristics and the specific treatment methods employed. Primary and activated sludge characteristics are reported by Tchobanoglous et al. (2014) as shown in Table 1.2. Generally, sewage sludge contains a mixture of inorganic and organic components. Organic matter consists primarily of carbohydrates, proteins, fats, and other biodegradable compounds. The high organic content makes sewage sludge suitable for biological treatment processes such as anaerobic digestion (Khanal, 2008d).

Anaerobically digested sludge retains essential nutrients as nitrogen (N) and phosphorus (P), which can be recovered and reused as fertilizers. This underscores anaerobic digestion not only as an effective method for reducing waste but also as a means of enhancing nutrient recovery. However, uncontrolled land application poses risks of eutrophication that result from excess nitrogen and phosphorus in aquatic systems. Proper management and regulation are therefore essential to maximize the benefits of nutrient recovery while minimizing environmental impacts.

Heavy metals are elements that naturally exist in the environment, typically identified by their high densities (above 4 g/cm^3), or atomic masses (Tchounwou et al., 2012; Vu, 2017; Yeşil, 2021). When these metals are found in concentrations under 10 mg/L, they are considered trace elements (Tchounwou et al., 2012; Yeşil, 2021). Trace elements and heavy metals commonly include metals such as lead (Pb), copper (Cu), cadmium (Cd), and zinc (Zn), which can create environmental and health risks if not managed appropriately (Inglezakis et al., 2014).

Table 1.2. Primary and waste activated sludge characteristic (Tchobanoglous et al., 2014)

Parameters	Primary Sludge	Activated Sludge
Total dry solids (TS), %	1-6	0.4-1.2
Volatile solids (% of TS)	60-85	60-85
Grease and fats (% of TS)	5-8	5-12
Protein (% of TS)	20-30	32-41
Nitrogen (N, % of TS)	1.5-4	2.4-5
Iron (not as sulfide)	2-4	-
pH	5.0-8.0	6.5-8.0
Alkalinity (g/L as CaCO3)	0.5-1.5	0.58-1.1
Energy Content (MJ/kg VSS)	23-29	19-23
K_2O (% of TS)	0-1	0-3
P_2O_5 (% of TS)	0.8-2.8	1.5-4

Due to their persistence, heavy metals do not decompose in natural surroundings, resulting in their buildup over time and posing significant threats (Vu, 2017; Yeşil, 2021). Since they are not biodegradable and dissolve easily in water, their transition into the human body is quite easy. Their harmful effects on human body are also well known (Buruiana et al., 2015; Kiran et al., 2022).

Pathogens, including bacteria, viruses, and parasites, are typically present in sewage sludge. Sewage sludge should be stabilized to prevent putrefaction and remove pathogens. Therefore, necessary treatment operations such as "*Standards for the Use or Disposal of Sewage Sludge"* and "*Process to significantly-further reduce pathogens(PFRP-PSRP)"* needs to be employed to mitigate health risks. These standards identify the limit values and describe detailed mitigation methods for pathogens (EPA, 1993, 2005). Sewage sludge may also contain emerging contaminants such as pharmaceuticals, microplastics, and other pollutants, reflecting the increasing complexity of modern wastewater streams (Mailler et al., 2014).

The high moisture content of sewage sludge, often exceeding 95% in untreated forms, complicates handling and disposal, necessitating dewatering and pretreatment processes (Ghangrekar, 2022; Tchobanoglous et al., 2014). Moreover, its heterogeneous composition poses challenges for uniform treatment and disposal methods, emphasizing the need for tailored solutions.

1.1.3. Management

From an engineering perspective, the primary goal of sludge management is to reduce the mass and volume of solids before transportation and final disposal. Management of sewage sludge is a multi-dimensional challenge that involves thickening, stabilization, dewatering and ultimate disposal. A sustainable sludge management also involves utilization of stabilized sludge in an environmentally and economically sound manner (Kiselev et al., 2019; Tyagi & Lo, 2013; Yesil et al., 2021b).

Key sludge management strategies include landfilling, anaerobic digestion, composting, and thermal processes (Tchobanoglous et al., 2014). Traditional methods for sludge disposal, such as landfilling and incineration (Adar et al., 2016), are increasingly criticized due to their environmental and regulatory concerns (Inglezakis et al., 2014). Among these, landfilling is one of the most primitive methods, involving the accumulating of waste in designated areas. Despite its environmental drawbacks, landfilling remains widely used, particularly in developing countries, due to its low cost and simplicity.

Anaerobic digestion (AD) is a well-established biological treatment process that decomposes organic matter under anaerobic conditions to produce biogas (a renewable energy source) and a stabilized sludge product (Cao & Pawłowski, 2012). This method has gained widespread acceptance for its dual role in energy recovery and waste stabilization. Composting converts sludge into a nutrient-rich organic fertilizer, suitable for agricultural applications. However, heavy metals and other emerging contaminants may limit its widespread usage (Kiselev et al., 2019). Thermal processes and advanced technologies and innovations such as incineration, pyrolysis, gasification, and hydrothermal carbonization are emerging as promising solutions for transforming sewage sludge into biofuels, biochar, or other value-added products (Adar et al., 2016; Chang et al., 2020; Tyagi & Lo, 2013).

Figure 1.2 shows the share of sewage sludges originating from urban WWTPs in European Countries and Türkiye (Eurostat, 2024)

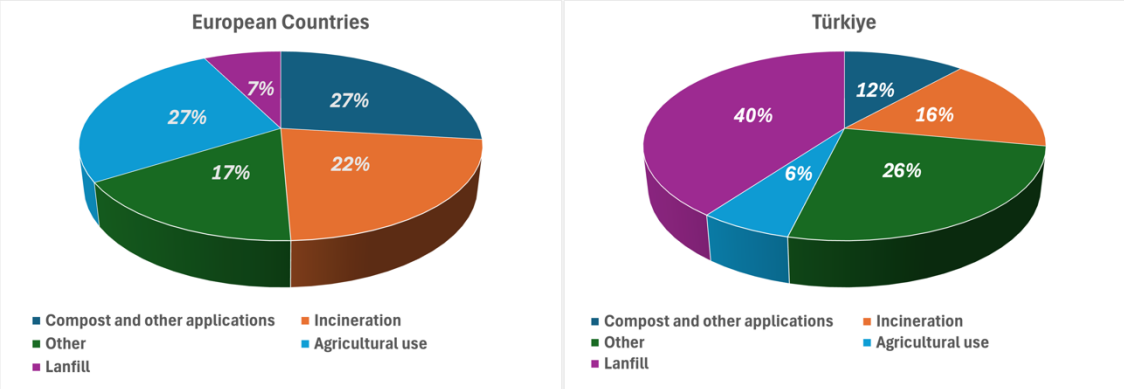

Figure 1.2. Urban sewage sludge disposal in 2022 (Eurostat, 2024)

The share of agricultural use, incineration and composting of sewage sludge is higher in European Countries (Figure 1.2). In contrast, one of the common sludge disposal method is landfilling in Türkiye (Figure 1.2). This highlights the significance of effective sewage sludge management in Türkiye.

Landfilling is becoming less favorable in European Countries due to space constraints, stricter environmental regulations, and greenhouse gas emissions from decomposing organic matter (Briard et al., 2018). Meanwhile, incineration of sludge is an effective method for volume reduction and energy recovery. However, it often requires costly air pollution control systems to mitigate the release of harmful emissions, such as dioxins and furans (Demirbas et al., 2017; Inglezakis et al., 2014).

Figure 1.3 illustrates a generalized sludge processing flow diagram (Tchobanoglous et al., 2014). Sludge processing encompasses not only the treatment of sewage sludge but also its final disposal or utilization. Each step contributes to comprehensive management of sludge, maximizing resource recovery while minimizing environmental impact (Figure 1.3).

The future of sludge management lies in adopting integrated approaches that combine resource recovery, waste minimization, and environmental protection (Yesil et al., 2021b). For example, AD coupled with nutrient recovery technologies such as struvite precipitation, can help recover both energy and valuable fertilizers from sludge. Furthermore, the application of pretreatment methods, such as ultrasonication, can

enhance sludge biodegradability and improve the efficiency of subsequent treatment processes (Yeşil, 2021).

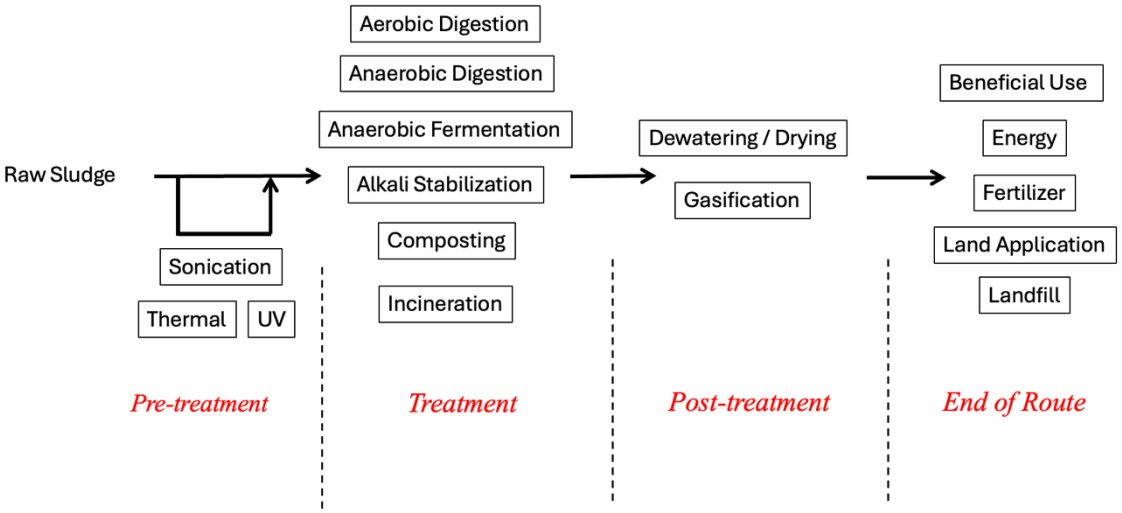

Figure 1.3. Generalized sludge processing flow diagram - Adopted from Tchobanoglous et al. (2014)

1.2. Anaerobic Digestion-Fermentation

AD is a biochemical process consisting hydrolysis, acetogenesis, acidogenesis, and methanogenesis enabling the breakdown of organic materials in the absence of oxygen, producing biogas and stable sludge (Harikishan, 2008a; Murphy & Thanasit, 2013). Whereas anaerobic fermentation process involves steps up to acidogenesis and produces valuable organic acids (Zacharof & Lovitt, 2013). Conversion of complex organic matters to valuable products such as biogas, stabilized sludge or organic acids, make anaerobic digestion or anaerobic fermentation processes a cornerstone of sustainable waste management, widely applied to sewage sludge, agricultural residues, food waste, and industrial organic waste. In the context of sewage sludge, anaerobic digestion not only stabilizes the waste but also produces valuable products such as methane and intermediate volatile fatty acids. Methane in biogas can be purified and used as an energy source and generated VFAs can be used as precursors for production of other valuable products (Lee et al., 2014), contributing to renewable energy production and reducing greenhouse gas emissions (Harikishan, 2008a; Khanal, 2008d).

1.2.1. Stages of anaerobic digestion

Anaerobic digestion is a multi-stage process (Figure 1.4), with each stage driven by specific microbial communities working in synergy.

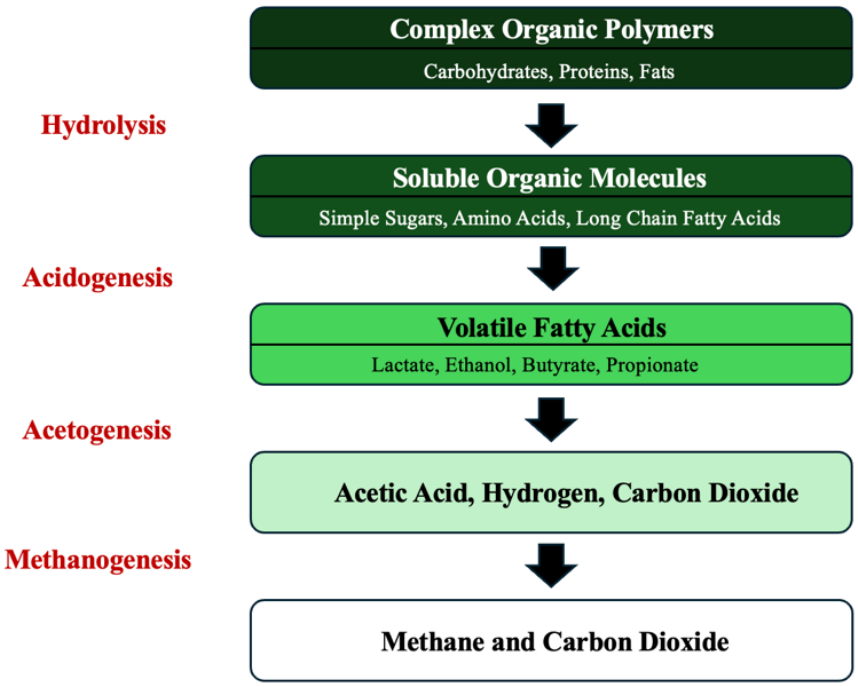

Figure 1.4. Anaerobic fermentation-digestion pathway of organic material - Adopted from Ghangrekar (2022)

Hydrolysis is the first step in the degradation process, involving the breakdown of complex macromolecules such as carbohydrates, proteins, and lipids into simpler, soluble monomers like sugars, amino acids, and fatty acids (Khanal, 2008d). Hydrolysis is facilitated by extracellular enzymes, including cellulases, proteases, and lipases, which are produced by hydrolytic microorganisms (Vavilin et al., 2008). Complex substrates like sewage sludge, particularly those with high lignocellulosic content, can hinder hydrolysis (Bochmann & Montgomery, 2013). Pretreatment techniques such as ultrasonication, thermal treatment, and chemical conditioning are often applied to enhance this stage by speeding up the hydrolysis step (Bochmann & Montgomery, 2013; Nguyen et al., 2021). Hydrolysis has significant role in AD process efficiency. It often dictates the rate of the entire anaerobic digestion process, it is considered the rate-limiting

step, particularly for substrates with high particulate content (Batstone, 2006) (Zhen et al., 2017).

In acidogenesis stage, the monomers produced during hydrolysis are fermented by acidogenic bacteria to produce alcohols, VFAs, hydrogen, and carbon dioxide (Batstone, 2006; Laiq Ur Rehman et al., 2019). Acidogenic microorganisms metabolize soluble compounds through fermentation pathways, generating byproducts such as acetate, butyrate, and propionate (Richard et al., 2019). Hydrogen gas and carbon dioxide are also produced during this phase, acting as intermediates for downstream processes. While VFAs are essential intermediates in the AD process, their accumulation can lead to acidification, reducing the overall process efficiency if not managed properly (Khanal, 2008b).

The products of acidogenesis are further converted into acetic acid, hydrogen, and carbon dioxide by acetogenic bacteria. Acetogenesis bridges acidogenesis and methanogenesis, ensuring the production of substrates that methanogenic archaea can utilize (Mohammad Mirsoleimani Azizi et al., 2021). This stage is particularly sensitive to hydrogen partial pressure, as high concentrations of hydrogen inhibit acetogenic activity (Batstone et al., 2002). The relationship between acetogens and methanogens is critical for maintaining process stability, as methanogens consume hydrogen and acetic acid, preventing their accumulation (Khanal, 2008b).

Methanogenesis is the final stage, where methanogenic archaea convert acetic acid and hydrogen to methane (CH_4) and carbon dioxide (CO_2) (Fang, 2015). There are two main pathways for methane production: Acetoclastic methanogenesis (utilizing acetic acid) and hydrogenotrophic methanogenesis (using hydrogen and carbon dioxide) (Richard et al., 2019). Methanogens are highly sensitive to changing environmental surroundings, particularly pH, temperature, and inhibitory compounds (Khanal, 2008c). Their performance largely dictates the overall biogas yield and process efficiency (Lohani & Havukainen, 2018). These stages operate in a delicate balance, with the efficiency of each stage influencing the subsequent ones. Disruptions in any stage, whether due to environmental factors or inhibitory compounds, can lead to reduced biogas production and process instability (Khanal, 2008c; Lohani & Havukainen, 2018).

1.2.2. Influence of environmental factors on anaerobic digestion

1.2.2.1.Alkalinity and pH

Maintaining an optimal pH (6.8–7.2) is crucial for the effective operation of AD, as it ensures microbial activity and digester stability (Tchobanoglous et al., 2014). Methanogens, which are highly sensitive to pH, thrive within a narrow range of 6.7–7.4, while acid-forming bacteria are active across a broader pH spectrum (Adhikari, 2006). Excessive production of VFAs can depress the pH, creating an imbalance that favors acidogenic bacteria over methanogens (Khanal, 2008b). Alkalinity, primarily provided by bicarbonates, acts as a reservoir to resist rapid pH changes and maintain the balance necessary for optimal microbial activity (Murphy & Thanasit, 2013). To prevent acidification and maintain equilibrium, buffering agents such as bicarbonates are commonly used to neutralize excess acids and stabilize the system. A stable pH not only safeguards methanogenic activity but also reflects overall system health and ensures optimal performance, typically near a pH of 7.0.

1.2.2.2.Temperature

Temperature plays a vital role in anaerobic digestion, influencing microbial growth, enzymatic activity, and the rates of hydrolysis and methane production (Khanal, 2008c). Digesters can operate within three temperature regimes: Psychrophilic (10–20°C), mesophilic (25–40°C), and thermophilic (45–65°C) (Khanal, 2008c; Murphy & Thanasit, 2013). Psychrophilic digestion operates at lower temperatures, with slower reaction rates but lower energy input requirements (Mao et al., 2015; Nie et al., 2021). Mesophilic digestion, the most commonly used regime, offers a balance of stability and efficiency, with optimal performance near 36°C (Khanal, 2008c). Most acid-forming microorganisms thrive under mesophilic conditions, while thermophilic digestion provides higher reaction rates and improved pathogen destruction, with methanogens performing optimally at around 55°C (Mao et al., 2015). However, the thermophilic regime demands significant energy input and exhibits lower stability compared to mesophilic digestion (Nie et al., 2021). In colder climates, where temperatures may drop below 20°C, substantial fluctuations can disrupt process performance (Mao et al., 2015; Petropoulos et al., 2017). To address this, external heating is often required to maintain

temperatures within the mesophilic range, typically above 25°C, ensuring stable and efficient operation.

1.2.2.3.Organic loading rate (OLR)

The organic loading rate (OLR), influenced by feed concentration and retention time, determines the food to biomass ratio within the liquid volume of reactor (Bedaso, 2019). The amount of organic material fed into the digester directly affects its efficiency. Overloading can lead to VFA accumulation and subsequent pH drops, while underloading may result in suboptimal biogas production (Franke-Whittle et al., 2014; Meegoda et al., 2018).

In a study by Jiang et al. (2013), synthetic food waste was fermented at varying organic loading rates (OLRs) (5–16 g TS/L.d). An increase in VFA concentration was observed as OLR rose from 5 g TS/L.d to 11 g TS/L.d (Jiang et al., 2013). Consequently, selecting an appropriate OLR is crucial for maintaining stable VFA production. According to the literature, an OLR of 5 g TS/L.d is recommended for mesophilic fermentation reactors (Strazzera et al., 2018).

1.2.2.4.Hydraulic retention time (HRT) and solid retention time (SRT)

The time substrate remains in the digester determines the extent of organic matter degradation (Mao et al., 2015; Nges & Liu, 2010). A longer HRT ensures more complete digestion but may reduce the economic viability of the process (Meegoda et al., 2018; Shi et al., 2017). Anaerobic digesters are designed with consideration of SRT and HRT to achieve effective degradation of volatile suspended solids (Nges & Liu, 2010; Tchobanoglous et al., 2014). SRT represents the average time solids remain in the reactor, while HRT refers to the time liquids are retained during the digestion process (Tchobanoglous et al., 2014). In a high-rate digester, the HRT and SRT are typically equal, both ranging between 15 and 30 days (Khanal, 2008a). Variations in SRT can influence the extent of metabolic reactions, including hydrolysis, fermentation, and methanogenesis, within the digester (Nges & Liu, 2010). Operating below the minimum required SRT can compromise these reactions, leading to incomplete digestion (Nges & Liu, 2010). Fortunately, this failure can be used to stop methanogenesis step to be able to produce VFAs via anaerobic fermentation (Yesil et al., 2021b).

1.2.3. Inhibition

Inhibitory compounds such as ammonia, sulfides, heavy metals, and antibiotics can disrupt microbial activity (Batstone et al., 2002; Rajagopal et al., 2013; Yeşil, 2021; Zielińska & Cydzik-Kwiatkowska, 2024). Effective pretreatment and pH control strategies are often employed to mitigate these effects (Yesil et al., 2021a). Inhibition is a critical challenge in anaerobic digestion, arising from various chemical and operational factors. Ammonia is produced during the degradation of nitrogen-rich compounds such as proteins (González-Fernández & García-Encina, 2009). Free ammonia is particularly toxic to methanogens, disrupting their enzymatic activity and reducing methane production (Bai et al., 2017; Batstone et al., 2002). Excessive VFA accumulation, often due to imbalances in hydrolysis or acidogenesis, can lower the pH, inhibiting methanogens and leading to process failure (Batstone et al., 2002; Fang, 2015; Khanal, 2008b; Li & Qiao, 2015).

Hydrogen sulfide (H_2S), which is produced by sulfate-reducing bacteria, is highly toxic to methanogens and can also corrode digester infrastructure (Batstone et al., 2002; Choudhury et al., 2019). Metals such as copper (Cu) and zinc (Zn) can bind to microbial enzymes, inhibiting their activity (Yeşil, 2021). Micropollutants, including pharmaceuticals and pesticides, also pose emerging challenges for sludge digestion (Zielińska & Cydzik-Kwiatkowska, 2024). The presence of oxygen disrupts anaerobic conditions, particularly affecting obligate anaerobes like methanogens (Tchobanoglous et al., 2014). Understanding these inhibitory factors and implementing mitigation strategies, such as pH control, and pretreatment is essential for enhancing the resilience and efficiency of anaerobic digestion systems.

1.3. Volatile Fatty Acid Generation using Anaerobic Fermentation

VFAs are short-chain organic acids, primarily including acetic, propionic, and butyric acids, produced during the acidogenesis and acetogenesis stages of anaerobic digestion (Richard et al., 2019). These acids play a crucial role as intermediates in the anaerobic fermentation process, serving as precursors for methane generation during methanogenesis. However, beyond their role in biogas production, VFAs have emerged

as valuable platform chemicals with applications in various industrial sectors (Lee et al., 2014).

1.3.1. Importance of VFA recovery

The recovery of VFAs from anaerobic fermentation processes have emerged as a critical area of focus due to their significant economic and environmental benefits (Zacharof & Lovitt, 2013). These organic acids, produced during the anaerobic breakdown of organic matter, offer a diverse range of applications across industries while contributing to the principles of a circular economy and sustainable waste management practices (Agler et al., 2011; Swarnima Agnihotri et al., 2022). VFAs are versatile chemicals that play an integral role in multiple fields. In the bioplastics industry, they serve as essential feedstock for the production of polyhydroxyalkanoates (PHAs), biodegradable polymers that address the growing environmental challenges posed by synthetic plastics (Lee et al., 2014). Similarly, their role in bioenergy production is noteworthy, as VFAs can be converted into biofuels through advanced processes such as microbial electrosynthesis and catalytic conversion (Agler et al., 2011; Zacharof & Lovitt, 2013). Beyond energy and materials, VFAs are invaluable in the food and pharmaceutical industries (Baird & Cann, 2012; Zacharof & Lovitt, 2013). Acetic and propionic acids, for example, are widely utilized as preservatives, flavor enhancers, and chemical intermediates, reflecting their broad utility (Zacharof & Lovitt, 2013). Beyond their applications, VFA recovery aligns with enhanced resource efficiency and sustainability of environment. Selective recovery of these compounds enables the valorization of organic waste streams such as sewage sludge, reducing dependence on fossil fuels for chemical production. In addition, VFA recovery aids in optimizing anaerobic fermentation process via eliminating the possibility of the weak acid inhibition (Batstone et al., 2002; Lee et al., 2014). The environmental benefits of VFA recovery are equally compelling (S. Agnihotri et al., 2022). The recovery processes minimize the carbon footprint avoiding the use of new raw materials to produce VFAs (Velghe et al., 2021). Furthermore, the bio-products derived from VFAs contribute to decarbonization efforts in industries ranging from energy to manufacturing, supporting global climate goals (Valentino et al., 2021; Velghe et al., 2021). The integration of VFA recovery into industrial and environmental strategies underscores its importance as a tool for fostering economic growth while addressing

pressing environmental challenges. As research and development in this field continue to evolve, VFAs are poised to play an even greater role in shaping a sustainable future (Velghe et al., 2021).

1.4. Pretreatment Prior to Anaerobic Fermentation

Pretreatment is a critical step in anaerobic fermentation processes, aimed at enhancing the biodegradability of organic substrates and improving the overall efficiency of AD (Zhen et al., 2017). Pretreatment methods disrupt the structural integrity of complex organic materials, such as sewage sludge. This leads to easier biodegradation and thus increased VFA production during anaerobic fermentation, improved biogas yields during AD, and reduced HRT (Ariunbaatar et al., 2014; Hartmann & Ahring, 2006).

To optimize the anaerobic digestion/fermentation processes, a variety of pretreatment methods have been developed, each targeting specific mechanisms to enhance substrate degradation. These methods are critical for improving the digestibility of organic matter, increasing biogas production, or facilitating the recovery of valuable intermediates like VFAs (Harikishan, 2008b).

Mechanical pretreatment involves physical processes such as milling, grinding, or cutting, which reduce the particle size of the substrate and increase the surface area available for microbial attack (Kumar & Sharma, 2017; Meegoda et al., 2018). Among these techniques, ultrasonic pretreatment stands out for its ability to disrupt the cell walls of microorganisms in sewage sludge, thereby releasing intracellular organic matter and making it more accessible for digestion (Lizama et al., 2017).

Thermal pretreatment uses elevated temperatures, typically between 50–250°C, to solubilize organic material and break down complex polymers (Nguyen et al., 2021). This method significantly enhances sludge digestibility but comes with a high energy demand, which can be a limiting factor in its application (Harikishan, 2008b).

Chemical pretreatment involves the use of acids, alkalis, or oxidizing agents to degrade organic matter (Nguyen et al., 2021). Acidic pretreatment is particularly effective at breaking down lignocellulosic structures, making it well-suited for biomass-rich substrates (Nguyen et al., 2021). Alkaline pretreatment is also effective for substrates

containing lignocellulosic materials. Additionally, it enhances the buffering capacity of the system, which helps maintain stability during processing (Zhen et al., 2017).

Biological pretreatment relies on microbial consortia or enzymatic treatments to pre-digest organic material in an environmentally friendly manner (Ariunbaatar et al., 2014). Although this method avoids the high energy or chemical inputs associated with other techniques, it generally requires longer processing times, which can limit its industrial scalability (Meegoda et al., 2018; Tyagi & Lo, 2013).

For maximum efficiency, multiple pretreatment methods have been used together to harness the synergistic effects of multiple approaches (Ariunbaatar et al., 2014). Thermo-chemical or mechano-chemical combinations, for instance, offer improved substrate degradation and digestion efficiency, making them suitable for substrates with complex compositions (Kim et al., 2010; Strong et al., 2011).

The selection of the most appropriate pretreatment method depends on various factors, including the substrate's characteristics, the desired end products (such as biogas or VFAs), and economic and environmental considerations (Zhen et al., 2017). By tailoring pretreatment strategies to these parameters, the efficiency and sustainability of AD processes can be significantly improved (Ariunbaatar et al., 2014; Zhen et al., 2017).

Among many pretreatment methods, ultrasonic pretreatment (ultrasonication) is a mechanical method applied to sewage sludge for rapid disintegration of bacterial cells (Harrison, 1991). By applying high-frequency sound waves, ultrasonication disrupts the structural integrity of sludge particles through a phenomenon known as cavitation (Pilli et al., 2011). This process produces micron sized bubbles in the liquid medium, which collapse and release intense localized energy, leading to several beneficial effects (Kuttruff, 2012).

One of the primary outcomes of ultrasonication is cell lysis, where the ultrasonic waves break the cell walls of microorganisms within the sludge (Lizama et al., 2017; Pilli et al., 2011). This releases intracellular organic matter into the solution, making it more accessible for microbial degradation during digestion (Pilli et al., 2016). Additionally, ultrasonication disrupts sludge flocs, reducing particle size and enlarging the surface area available for enzymatic hydrolysis (Pilli et al., 2011). This enhanced surface area

accelerates the breakdown of organic material during digestion (Aldin et al., 2010; Lizama et al., 2017; Passos et al., 2014).

Another key benefit of sonication is improved solubilization (Bougrier et al., 2005). The treatment facilitates the breakdown of complex organic matter, such as proteins, carbohydrates, and lipids, making them readily available for microbial activity. This accelerates the hydrolysis stage of anaerobic digestion, which is often a rate-limiting step in the process (Aldin et al., 2010).

Ultrasonication increases both biogas yield and VFA production, reduces the HRT required for digestion, and enhances the overall efficiency of anaerobic processes (Liu et al., 2018). However, there are challenges associated with its implementation. The high energy demands of large-scale sonication can limit its economic feasibility (Aldin et al., 2010), and the process requires careful calibration of parameters such as, duration, frequency, and energy input, to balance efficiency with energy consumption while avoiding excessive substrate degradation (Aldin et al., 2010).

Despite these challenges, sonication has been extensively studied and proven to improve the biodegradability of sludge and enhance the performance of AD systems (Aldin et al., 2010; Lizama et al., 2017; Passos et al., 2014; Zerrouki et al., 2021). Its ability to increase the efficiency of substrate breakdown and promote resource recovery underscores its potential as a valuable pretreatment method in sustainable waste management practices.

1.5. Mathematical Modeling

Modeling is a crucial tool for understanding, analyzing, and optimizing AD processes (Yu et al., 2013). It provides valuable insights into the dynamics of biological, chemical, and physical phenomena, enabling predictions of system behavior under varying operational conditions (Batstone, 2006). Effective modeling supports informed decision-making in system design, operation, and control, thereby increasing the efficiency and sustainability of sewage sludge treatment processes (Batstone & Rodríguez, 2015; Fang, 2015; Sharma, 2008).

There are several approaches to modeling AD, each with distinct applications (Batstone & Rodríguez, 2015; Fang, 2015). Empirical models are among the simplest structure, relying on experimental data to describe system behavior (Batstone & Rodríguez, 2015;

Fang, 2015). While these models are computationally easy to implement, they are limited in their ability to generalize beyond the specific conditions of the experimental dataset (Fang, 2015). Furthermore, empirical models require experimental setup to generate a reliable formula which means extra costs and time (Yu et al., 2013).

For a more detailed understanding, kinetic models are often employed. These models capture the rates of biological and chemical reactions involved in AD, such as hydrolysis, acidogenesis, acetogenesis, and methanogenesis (Batstone, 2006; Yu et al., 2013). By utilizing differential equations, kinetic models describe substrate degradation and microbial growth dynamics, offering a mechanistic perspective on the process (Batstone et al., 2002; Yu et al., 2013). This makes them valuable for exploring how various parameters, such as inhibition, pH, or substrate composition, influence digestion performance (Batstone et al., 2002; Sharma, 2008).

Mathematical and computational models provide even greater complexity and comprehensiveness. Frameworks like the Anaerobic Digestion Model No.1 (ADM1) integrate biochemical reactions, physicochemical interactions, and transport phenomena into a unified model (Batstone et al., 2002). These models often require advanced computational tools to solve the complex equations they generate, making them particularly useful for large-scale or highly dynamic systems. Their ability to simulate sophisticated interactions within the digestion process makes them indispensable for optimizing system performance in real-world applications (Batstone, 2006).

Each modeling approach plays a critical role in advancing the understanding and optimization of AD processes. The choice of model depends on the specific objectives, system scale, and available data, ensuring that the modeling framework aligns with the operational and research goals of the AD system (Fang, 2015).

Mathematical modeling provides a systematic framework to capture the complex dynamics of AD processes. By describing the detailed interactions among substrates, microorganisms, and environmental conditions; these models play a pivotal role in advancing the understanding and optimization of AD systems. A fundamental component of mathematical modeling is the incorporation of mass balances (Eqn. 1.1). These models ensure the conservation of mass within the system by tracking substrates, intermediates, and products throughout the process (Yu et al., 2013). Temporal changes in the

concentrations of key compounds are represented through differential equations, enabling precise predictions of system behavior over time (Fang, 2015).

$$Accumulation = Input - Output \pm Reaction \quad (1.1)$$

Another critical aspect of mathematical modeling is reaction kinetics, which define the rates of substrate degradation, microbial growth, and potential inhibitory mechanisms (Sharma, 2008). While many models employ first-order kinetics (Eqn. 1.2) to describe disintegration and hydrolysis, they utilize Monod-type kinetics (Eqn. 1.3) to determine microbial activity, often incorporating modifications to account for specific inhibitory effects such as those caused by excessive VFAs or ammonia.

$$\frac{dC_i}{dt} = -k_h \,.\, C_x \quad (1.2)$$

where C_i, C_x, k_h, t, represent the concentration of component i, concentration of biomass x, rate constant of related reaction and time, respectively (Eqn. 1.2).

$$\rho = k_m \,.\, Y.X.\frac{S}{k_{s+S}} \quad (1.3)$$

where ρ, k_m, Y, X, S, k_s represent reaction rate, maximum specific uptake rate, yield coefficient, biomass, substrate and half-saturation constant, respectively (Eqn. 1.3).

Environmental factors such as temperature and pH are also integral to mathematical models. These parameters significantly influence microbial activity and reaction rates, and dynamic models are particularly effective for simulating variations in environmental conditions (Batstone et al., 2002). This makes mathematical modeling an essential tool for analyzing system responses to fluctuating operational parameters.

For mathematical models to be reliable and applicable, calibration and validation are essential steps (Panaro et al., 2021). Calibration involves adjusting model parameters using experimental data to ensure they accurately reflect real-world systems (Panaro et al., 2021; Refsgaard & Storm, 1996). Validation with independent datasets further ensures that the model is robust and can generalize across different scenarios (Panaro et al., 2021).

By integrating mass balances, reaction kinetics, and environmental influences, mathematical models provide a foundation for designing, controlling, and optimizing AD

processes. Mathematical tools provide ability to researchers and engineers to foresee system performance, evaluate potential improvements, and develop sustainable solutions for waste management and resource recovery.

1.5.1. Anaerobic Digestion Model No.1 (ADM1)

ADM1 is a standardized mathematical model developed by the International Water Association (IWA) to simulate the biochemical and physicochemical processes in anaerobic digesters (Batstone et al., 2002). ADM1 is widely recognized for its comprehensive structure and applicability to various substrates and system configurations. ADM1 mostly uses concentration while its simulations-calculations. Table 1.3 shows wide-range of units that is used by ADM1.

Table 1.3. Units (Batstone et al., 2002)

Measure	**Units**
Concentration	kg COD/m^3
Concentration (non-COD)	kmole C /m^3
Concentration (nitrogen non-COD)	kmole N/m^3
Pressure	bar
Temperature	K
Energy	J (kJ)
Time	d (day)

1.5.1.1.Dimensions of ADM1

ADM1 captures the complexity of AD through its detailed *components* (Table 1.4), *reaction pathways* (Figure 1.5), and *time*-dependent dynamics. ADM1 stands as a significant framework in the field of AD, offering a detailed and dynamic approach to understanding and simulating the complex biological, chemical, and physical processes involved. Its design integrates a range of components, reaction pathways, and time-

dependent dynamics, making it one of the most comprehensive tools available for modeling AD systems.

Table 1.4. Liquid phase components (Batstone et al., 2002)

Particulate	**Soluble**
X_c, Composite	S_{su}, Sugars
X_{ch}, Carbohydrates	S_{aa}, Amino acids
X_{pr}, Proteins	S_{fa}, Long-chain fatty acids
X_{li}, Lipids	S_{va}, Total valerate
X_{su}, Sugar degraders	S_{bu}, Total butyrate
X_{aa}, Amino acid degraders	S_{pro}, Total propionate
X_{fa}, Long-chain fatty acid degraders	S_{ac}, Total acetate
X_{c4}, Valerate and butyrate degraders	S_{h2}, Hydrogen
X_{pro}, Propionate degraders	S_{ch4}, Methane
X_{ac}, Acetate degraders	S_{IC}, Inorganic carbon
X_{h2}, Hydrogen degraders	S_{IN}, Inorganic nitrogen
X_I, Particulate inerts	S_I, Soluble inerts

At its foundation, ADM1 encompasses a wide array of state variables that represent the complexity of the digestion process. These variables include particulate and soluble substrates, microbial biomass, and critical intermediate products such as VFAs, hydrogen, and methane (Batstone et al., 2002). Each of these variables plays a vital role in the system, reflecting the interactions and transformations that occur during digestion.

The model goes further by categorizing microbial populations into hydrolytic, acidogenic, acetogenic, and methanogenic groups (Batstone et al., 2002). This classification enables ADM1 to represent the distinct metabolic roles and interactions of these microbial communities, each contributing to the sequential stages of AD.

Beyond its detailed representation of components, ADM1 incorporates an extensive range of reactions that drive the AD process (Figure 1.6). Biochemical reactions, such as

hydrolysis (the breakdown of complex organic matter into simpler compounds), acidogenesis (the production of VFAs and alcohols), acetogenesis (the conversion of VFAs into acetate, hydrogen, and carbon dioxide), and methanogenesis (the final step where methane and carbon dioxide are produced), are central to the model (Figure 1.5).

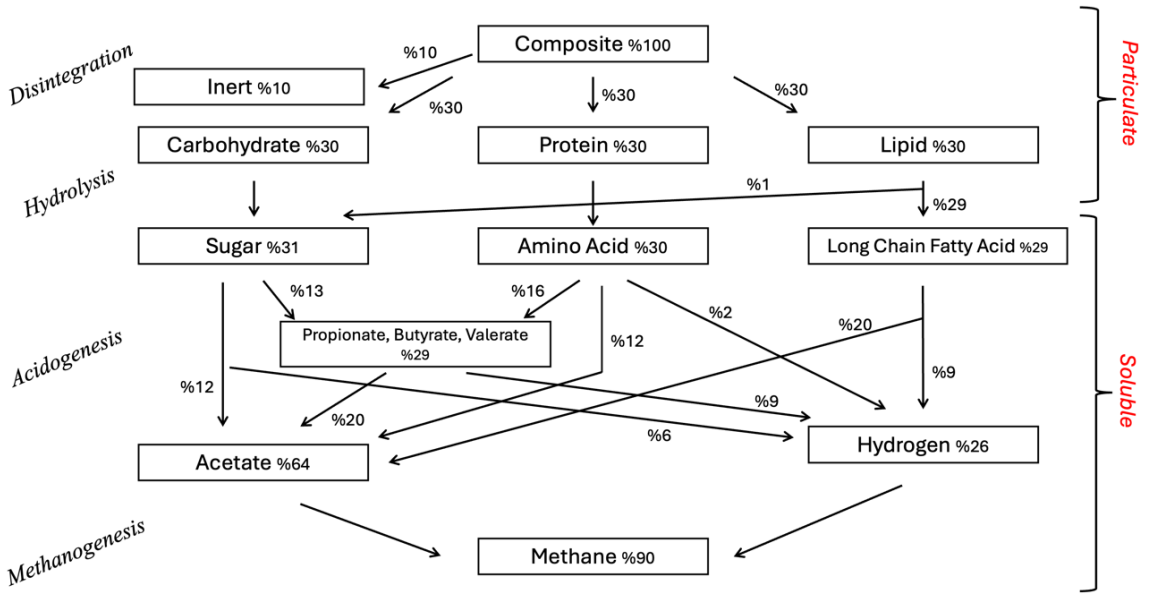

Figure 1.5. Distribution of composite - Adopted from Batstone et al. (2002)

These reactions are coupled with critical physicochemical processes, such as gas-liquid transfer (Figure 1.6), which governs the exchange of methane and carbon dioxide between the liquid and gaseous phases, and pH buffering, which stabilizes the system against acidification (Batstone et al., 2002). The kinetics of these reactions are described using a combination of first-order, Monod, and inhibition-based equations, enabling the model to account for substrate availability, microbial growth rates, and inhibitory effects caused by compounds such as ammonia or VFAs.

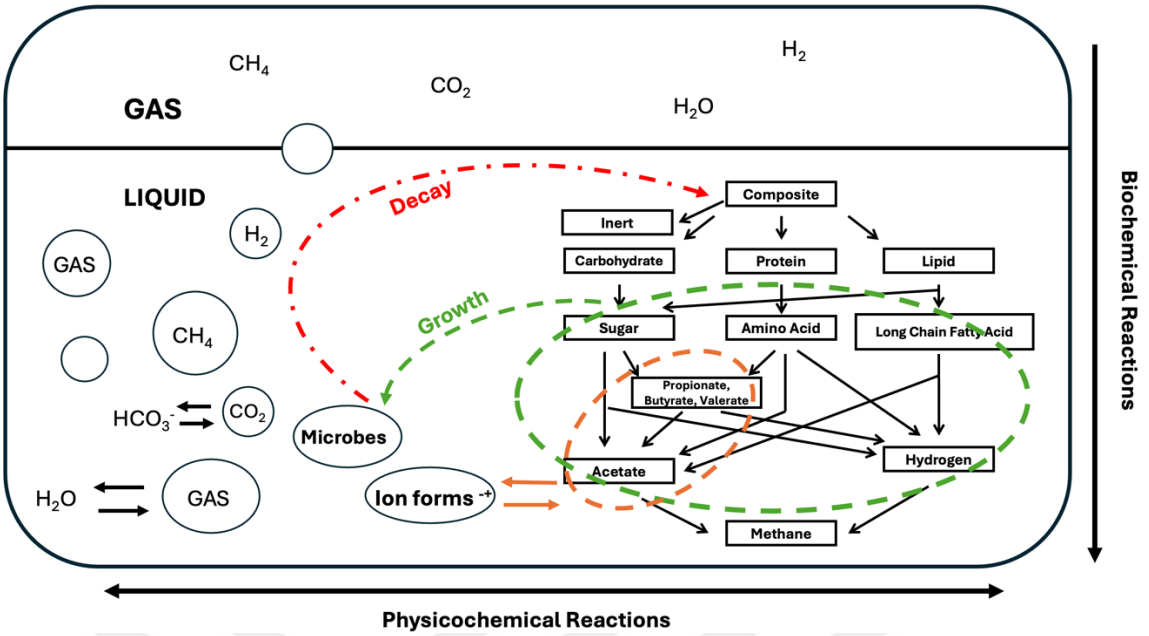

Figure 1.6. Reactions in anaerobic fermentation in reactor - Adopted from Batstone et al. (2002)

A key strength of ADM1 lies in its dynamic nature. Equations 1.4 and 1.5 are differential equations that used by ADM1 that proves this dynamic nature (Batstone et al., 2002). Unlike static models that provide a snapshot of system behavior, ADM1 operates over time, simulating the temporal evolution of system variables under changing conditions (Figure 1.7).

$$\frac{dS_{liq,i}}{dt} = \frac{q_{liq}}{V_{liq}}\left(S_{in,i} - S_{liq,i}\right) + \sum_{j=1-19} \rho_j \, v_{i,j}; \quad i = 1-12. \tag{1.4}$$

$$\frac{dX_{liq,i}}{dt} = \frac{q_{liq}X_{in,i}}{V_{liq}} - \frac{X_{liq,i}}{t_{resX} + {V_{liq}}/{q_{liq}}} + \sum_{j=1-19} \rho_j \, v_{i,j}; \quad i = 13-24 \tag{1.5}$$

where $S_{liq,i}$ (Eqn. 1.4) represents the concentration of component i in the digester, $X_{liq,i}$ (Eqn. 1. 5) represents the concentration of biomass in the digester. $S_{in,i}$ and $X_{in,i}$ are influent concentration of component and biomass i, respectively (Eqn. 1.4 and 1.5). Q_{liq} and V_{liq} represents liquid flow rate and volume of the anaerobic digestion system (Eqn. 1.4 and 1.5). Each ρ_j exemplifies the reaction rate of process j, and each $v_{i,j}$ exemplifies the

biochemical rate coefficients of component *i* for process *j* as used in Eqn. 1.4 and 1.5. T_{resX} represents the residence time of solid components above HRT in the reactor (Eqn. 1.5). These liquid phase equations are given in order to explain the dynamic nature of the ADM1 (Figure 1.7). Gas phase equations are also included in ADM1 (Batstone et al., 2002).

This dynamic capability allows the model to respond to variations in operational parameters, such as changes in substrate loading rates, temperature, or HRT (Batstone et al., 2002). By adjusting time steps based on system dynamics, ADM1 ensures accurate and efficient simulations, making it particularly valuable for analyzing transient states or optimizing system performance during fluctuating conditions (Batstone et al., 2002).

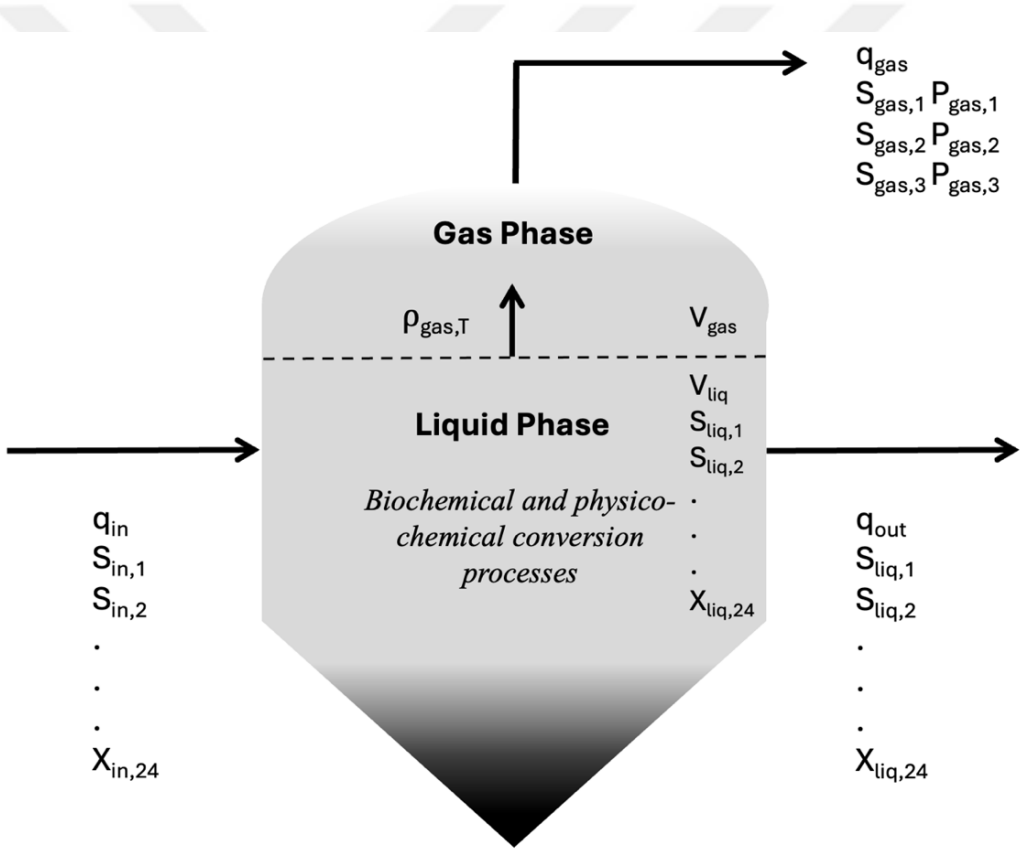

Figure 1.7. Dynamic environment of ADM1 - Adopted from (Batstone et al., 2002)

ADM1's adaptability further enhances its utility (Batstone et al., 2006). While originally developed for municipal wastewater treatment, the model can be tailored to accommodate a variety of substrates, including agricultural residues, industrial waste, or co-digestion systems. Researchers and engineers can modify the model to include additional processes

or adapt its parameters to reflect specific operational scenarios (Batstone et al., 2006). This flexibility has positioned ADM1 as a cornerstone for both academic research and practical applications, enabling advancements in the design, operation, and optimization of AD systems (Batstone et al., 2002).

Despite its complexity, ADM1 provides a structured and robust framework for understanding the multifaceted nature of AD. Its ability to integrate components, reactions, and time-dependent dynamics offers a powerful platform for addressing challenges in waste treatment and resource recovery. As the demand for sustainable waste management practices continues to grow, ADM1 remains an indispensable tool, driving innovation and efficiency in the field of AD.

1.5.1.2.Limitations of ADM1

ADM1, like any model, comes with limitations that must be considered when applying it to real-world systems. ADM1 relies on numerous parameters, many of which are challenging to measure or estimate accurately (Batstone et al., 2015). Uncertainty in these parameters can lead to variability or reduced reliability in the model's predictions, posing a barrier to its application in systems where precise data is unavailable (Batstone et al., 2015). The assumptions underlying ADM1 also limit its applicability in some cases (Batstone et al., 2015). The model assumes ideal mixing and homogeneous conditions, which may not align with the heterogeneous environments typically found in full-scale digesters (Batstone et al., 2002). Additionally, ADM1 simplifies microbial interactions and inhibition mechanisms, potentially overlooking the more intricate dynamics of anaerobic digestion (Batstone et al., 2002). Lastly, the application range of ADM1 presents another constraint. The model was originally developed for municipal wastewater treatment systems, meaning it may require adaptation to handle unconventional substrates, such as industrial waste, agricultural residues, or co-digestion systems (Mo et al., 2023). Anaerobic digestion of sewage sludge taken from municipal wastewater treatment systems that are operated at extended aeration mode may not be well modeled using ADM1 (Batstone et al., 2015). In brief, without modification, its applicability to such substrates may be limited.

Despite these limitations, ADM1 remains a foundational framework in AD modeling. Its versatility allows users to customize and extend the model to include additional processes

or adapt it to specific operational conditions, making it a valuable tool for both research and practical applications (Batstone et al., 2006).

1.5.1.3. Modifications of ADM1 for AD of pretreated sewage sludge and pH control in digesters

In recent years, many studies focused on modifying ADM1 to enhance its capability for assessing anaerobic digestion and fermentation processes, particularly for pretreated organic wastes. Souza et al. (2013) developed a model to evaluate the performance of a continuous anaerobic digester fed with thermally pretreated sewage sludge. Calibration of disintegration and hydrolysis coefficients was achieved using biochemical methane potential tests, and ADM1 was implemented with modifications proposed by Rosen et al. (2006); (Souza et al., 2013). Their findings were validated using laboratory-scale continuous digesters (Souza et al., 2013). Similarly, Ramirez et al. (2009) investigated the anaerobic digestion of thermally pretreated waste-activated sludge by employing a modified ADM1. The Contois model was used instead of first-order kinetics for disintegration and hydrolysis (Ramirez et al., 2009). The modified ADM1 incorporated new biochemical parameters for disintegration, as well as hydrolysis parameters for carbohydrates, proteins, and lipids (Ramirez et al., 2009). Calibration and validation were performed using experimental batch reactor data, demonstrating that the modified ADM1 could effectively evaluate the impact of pretreatment on anaerobic digestion (Ramirez et al., 2009).

Aldin et al. (2010) modeled the effects of sonication across a range of specific energy inputs on the anaerobic digestion of primary and waste-activated sludge. Their model excluded ammonia and pH inhibition for simplicity and estimated acetic acid utilization rates for waste-activated sludge, while utilization rates for acetic, butyric, and valeric acids were determined for primary sludge (Aldin et al., 2010). The outcomes in terms of methane and VFA concentrations were successfully predicted using modified ADM1, calibrated with batch biodegradability and gas production studies (Aldin et al., 2010).

Beyond pretreatment modeling, other research has explored the impact of pH control on anaerobic fermentation. Bai et al. (2015) modeled alkaline fermentation to examine its effects on VFA dynamics. Their study utilized simple Monod and non-inhibition equations, optimizing utilization rates to successfully simulate the effects of alkaline

conditions (Bai et al., 2015). Similarly, Huang et al. (2018) modeled acidogenic fermentation of sugar containing wastewater under acidic conditions by extending the ADM1 stoichiometric matrix to include ethanol, a fermentation product. They adjusted the stoichiometry for monosaccharides and butyrate utilization, and introduced ethanol utilization parameters based on experimental data (Huang et al., 2018). Their modified ADM1 was successfully calibrated to capture the effects of low-pH conditions on acidogenic fermentation (Huang et al., 2018).

1.6. Objective of the Study

While significant progress has been made in modeling either sludge pretreatment or pH controlled anaerobic fermentation (Aldin et al., 2010; Bai et al., 2015; Huang et al., 2018; Ramirez et al., 2009; Souza et al., 2013), no study has yet demonstrated the synergistic effects of these two factors. This study aimed to address this gap by modifying ADM1 to model pH controlled anaerobic fermentation of ultrasound-pretreated sewage sludge. Combining sludge pretreatment with pH controlled fermentation represents an emerging area of interest within the carboxylate platform. Modifying ADM1 to account for ultrasonic pretreatment under varying pH conditions could yield critical insights for optimizing VFA production. Capturing these interactions within ADM1 necessitates rigorous calibration against experimental data and subsequent validation to ensure model flexibility and reliability. The specific objective was to estimate individual VFA production in a continuous pH controlled fermentation system for both non-pretreated and ultrasonicated sewage sludge under acidic, control, and alkaline conditions. The modified ADM1 was calibrated using data from three continuous anaerobic fermenters (Yesil et al., 2021b) and subsequently validated with the experimental data by Yeşil (2021)(details in Section 2.2) demonstrating its robustness and potential applicability.

2. MATERIAL & METHOD

2.1. Experimental Data for Modeling

Yeşil (2021) carried out a series of experiments in order to evaluate the effects of bio-leaching, and volatile fatty acid (VFA) production in pH controlled anaerobic fermentation using ultrasound-pretreated sewage sludge. The sewage sludge was obtained from the activated sludge section of the Ataköy Advanced Biological Wastewater Treatment Plant (WWTP), in Istanbul, Türkiye, where the SRT was over 20 days (Yesil et al., 2021b).

Before anaerobic fermentation, the sludge underwent disintegration via ultrasound pretreatment (Yesil et al., 2021b). Ultrasonication was applied to 100 mL of raw sludge for 10 minutes using an ultrasonic generator (Specifications: 1 kW/L, 20kHz) (Yesil et al., 2021b). Fermentation of the pretreated sludges was conducted in three identical completely mixed reactors, each with a working volume of 1.3 L (including a 0.5 L head space) (Yesil et al., 2021b).

During start-up, the reactors were inoculated with an enriched fermentative population at an inoculum to substrate ratio 1:3, based on organic solids (Yesil et al., 2021b). Raw or pretreated sludge was fed into three identical reactors over two different operational periods: days 0-38 for non-treated sludge feeding and days 39-77 for ultrasound pretreated sludge feeding (Yesil et al., 2021b). Since this thesis modeled the experimental data starting from day 19, the operating periods were redefined as days 0–20 for non-pretreated sludge feeding and days 21–59 for ultrasound pretreated sludge feeding. Each reactor was operated at 35°C under acidic, control (neutral), or alkaline pH conditions in a semi-continuous feeding (Yesil et al., 2021b). The organic loading rate (OLR) was obtained at 1.17 kg VS/m^3.d, with a total solids (TS) content of 1.3%, and an solids retention time (SRT) of 4 days (Yesil et al., 2021b).

2.2. Experimental Data for Validation

The optimized model was validated using data collected by our group (Yeşil, 2021) from a laboratory-based experiment conducted previously as part of a PhD thesis. In this study, a 5 L continuously stirred tank reactor (CSTR) with a 2 L headspace was operated as a

fermentation-based anaerobic reactor under mesophilic (36±0.5°C) and alkaline (pH 9) conditions. The anaerobic reactor was semi-continuously fed with sewage sludge taken from Ataköy Advanced Biological WWTP, which was operating at a SRT of 20 days during the sludge collection period (Yeşil, 2021). While the reactor ran for a total of 280 days, only data from the first 47 days was used for model validation (Yeşil, 2021). This period (days 0–47) was divided into two distinct operational phases (days 0–11 and days 12–47) due to variations in OLR and SRT. Initially (days 0–11), the OLR and SRT were maintained at 6.81 kg COD/m^3·d (4.75 kg VS/m^3·d) and 7.4 days, respectively. From days 12 to 47, the OLR was reduced to 5.94 kg COD/m^3·d (4.15 kg VS/m^3·d), while the SRT was adjusted to 8 days (Yeşil, 2021).

2.3. Modeling of Anaerobic Fermentation of pH Controlled Ultrasound Pretreated Sewage Sludge through the Anaerobic Digestion Model No.1

In this study, lab-scale experimental data sets reported Yesil et al. (2021b); (Yeşil, 2021) by was used to optimize and validate the model ADM1 extended with the effect of pretreatment on VFA production efficiency.

2.3.1. Implementation of ADM1

The ADM1 was individually implemented for three identical pH levels (pH 5, pH 7, and pH 10) according to guidelines of Batstone et al. (2002) operating MATLAB version R2024a. The operating system of the computer was MacOS Sequoia 15.1.1. Codes were developed regarding to the original ADM1 model generated by (Batstone et al., 2002). Empirical upper and lower inhibition equation (Eqn. 2.1) were selected to predict the effects of inhibition on the three identical pH levels in the reactors (Batstone et al., 2002).

$$I = \frac{1 + 2 \times 10^{0.5(pH_{LL} - pH_{UL})}}{1 + 10^{(pH - pH_{UL})} + 10^{(pH_{LL} - pH)}} \quad (2.1)$$

The symbols pH_{LL} and pH_{UL} represents the lower and upper pH limits of the related bacteria (Eqn. 2.1). This empirical inhibition formula is used to quantify pH inhibition when both high and low pH conditions affect bacterial activity.

Remaining algebraic and differential equations such as process, gas transfer, and acid-base rates; inhibition, and mass balance were set according to ADM1.

2.3.1.1.Initial assumptions

The initial influent was assumed to consist of composite matter *(X_c)* and biomass *($X_{biomass}$)* due to the complicated characteristics of sewage sludge. The stoichiometric coefficients for the disintegration (Table 2.1) process were applied according to Rosen et al. (2006), who used ADM1 to simulate the anaerobic digestion (AD) of sewage sludge.

Table 2.1. Initial assumptions

Parameter	Value	Unit	Definition
Initial Influent *(X_c+$X_{biomass,total}$)*	6.63	kg COD/m^3	Influent of digesters
$f_{ch,Xc}$	0.2	-	Carbohydrate/composite
$f_{pr,Xc}$	0.2	-	Protein/composite
$f_{li,Xc}$	0.3	-	Lipid/composite
$f_{xi,Xc}$	0.2	-	Inert/composite
$f_{si,Xc}$	0.1	-	Soluble Inert/composite
X_{ch}, X_{pro}, X_{li}, X_I, S_I	0	kg COD/m^3	Particulate carbohydrate, protein, lipid, inert, and soluble inert
S_{su}	0.01	kg COD/m^3	Soluble sugar
S_{aa}, S_{fa}, S_{ac}, S_{pro}, S_{bu}, S_{va}	0.001	kg COD/m^3	Soluble amino acid, fatty acid, acetate, propionate, butyrate, and valerate
S_{H2}	10^{-8}	kg COD/m^3	Soluble hydrogen
S_{CH4}	10^{-5}	kg COD/m^3	Soluble methane
S_{IC}	0.04	kmole C /m^3	Soluble inorganic carbon

Considering that acidogenic and acetogenic fermentative bacteria can function over a wide range of pH range, the inhibition factor for all acidogenic and acetogenic bacteria *($pH_{ul,aa}$)* was increased from 5.5 to 8.5 (Huang et al., 2018).

At start-up of the AD process, soluble components are not expected to be present in the digester. Therefore, their initial concentrations were assumed to nearly zero in the system (Table 2.1).

The reactors were inoculated during at the initiation of the experiment. Therefore, all degraders-biomass *(X_{su}, X_{aa}, X_{fa}, X_{ac}, X_{pro}, X_{c4}, X_{h2})* were adjusted to 0.1 kg COD/m^3 prior to initializing the simulation.

2.3.1.2.Initial parameters

Physical parameters such as flow rate (q_{in}), liquid and gas volume of the reactors *(V_{liq}, V_{gas})*, solid retention time *(SRT)*, and temperature *(T)*; available steady-state input variables (Table 2.2) were set based on lab-scale experimental data (Yesil et al., 2021b).

Table 2.2. Initial variables of experiment modeled

Parameters	Value	Unit	Definition
q_{in}	$2x10^{-4}$	m^3/day	Flow rate
V_{liq}	$8x10^{-4}$	m^3	Volume of liqueur
V_{gas}	$5x10^{-4}$	m^3	Volume of gas
SRT	4	day	Solids retention time
T	308	K	Temperature
X_c	5.93	kg COD/m^3	Composite
S_{IN}	0.006	kmole N/m^3	Soluble inorganic nitrogen
S_{IN}	0.015	kmole N/m^3	Soluble inorganic nitrogen (Negral et al., 2015)

The positive effect of the pretreatment to ammonium concentration in raw secondary sludge was investigated by Negral et al. (2015). In their study, secondary sludge was ultrasonicated with almost same amount of energy with the experiment modeled in this

study. In this perspective, initial S_{IN} was estimated to increase from 0.006 to 0.015 kmole N/m^3 (Table 2.2) after pretreatment in line with the study by Negral et al. (2015).

There are some studies in the literature investigating VFA composition during anaerobic fermentation at different pH levels, which have shown that acetic acid is the dominant VFA under alkaline condition (Garcia-Aguirre et al., 2017; Li et al., 2017; Liu et al., 2012; Liu et al., 2014; Regueira et al., 2021; Shi et al., 2022). Therefore, stoichiometric coefficients of volatile fatty acids (VFAs) derived from amino acids ($f_{ac,aa}$, $f_{pro,aa}$, $f_{bu,aa}$, $f_{va;aa}$, $f_{h2,aa}$) were calculated (Appendix 1) according stoichiometric data from the study by Liu et al. (2012) for alkaline conditions, differing from the acidic and control conditions (Table 2.3).

Table 2.3. Modified stoichiometric parameter values of amino acid in the modified ADM1

Parameters	Modified Value	ADM1	Unit	Definition
$f_{ac,aa}$	0.65	0.40	-	Acetate/Amino acid
$f_{pro,aa}$	0.11	0.05	-	Propionate/Amino acid
$f_{bu,aa}$	0.11	0.26	-	Butyrate/Amino acid
$f_{va,aa}$	0.07	0.23	-	Valerate/Amino acid
$f_{h2,aa}$	0.06	0.06	-	Hydrogen/Amino acid

The effects of pretreatment and different pH conditions on fermentation are mostly related to hydrolysis, which is rate-limiting process in AD, and utilization rates (Aldin et al., 2010; Batstone et al., 2009; Huang et al., 2018; Ramirez et al., 2009; Vavilin et al., 2008; Vavilin et al., 1996). Therefore, during the initial stage, hydrolysis and utilization of VFAs' rate constants which are shown in Table 2.4 were optimized through trial and error based on the VFA results obtained from the experiment. Remaining initial parameters were adapted according to ADM1 original (Batstone et al., 2002).

2.3.2. Parameter optimization - tunning

Biochemical processes are quite significant for anerobic fermentation systems. Therefore, optimization of system was initiated with disintegration (k_{dis}) and hydrolysis rate constants ($k_{hyd,ch}$, $k_{hyd,ch}$, $k_{hyd,li}$) for three pH conditions in this study. As the optimization process advanced, utilization and half saturation rate constants of propionate ($k_{m,pro}$, $k_{s,pro}$), butyrate, and valerate ($k_{m,c4}$, $k_{s,c4}$) were also included in the optimization in order to achieve better results under acidic condition.

Table 2.4. Optimized parameters in the modified ADM1

Parameters	ADM1	pH 5		pH 7		pH 10	
		N	P	N	P	N	P
k_{dis} (day^{-1})	0.5	0.6	0.7	0.5	0.7	0.7	0.8
$k_{hyd,ch}$ (day^{-1})	10	0.015	0.09	0.012	0.06	0.08	0.8
$k_{hyd,pro}$ (day^{-1})	10	0.015	0.09	0.012	0.06	0.08	0.8
$k_{hyd,li}$ (day^{-1})	10	0.015	0.09	0.012	0.06	0.08	0.8
$k_{m,pro}$ (day^{-1})	13	4	4	*	*	*	*
$k_{s,pro}$ (day^{-1})	0.1	0.3	0.3	*	*	*	*
$k_{m,c4}$ (day^{-1})	20	7	7	*	*	*	*
$k_{s,c4}$ (day^{-1})	0.2	0.6	0.6	*	*	*	*

*(N: Non-treated, P: Pretreated, *: ADM1 original value)*

Wide parameter ranges were initially determined (from 0.1 to 1 day^{-1} for disintegration rate constants, from 0.001 to 20 $day^{-1}$for hydrolysis rate constants, from 3 to 30 day^{-1} for utilization rate constants, and from 0.05 to 0.8 day^{-1} for half saturation rate constants) by comparing model outcomes with experimental VFA results. Scientifically established

general system behaviors of anaerobic fermentation in related processes also supported the definition of these ranges. Subsequently, the ranges were narrowed and fine-tuned through multiple trials, an effective method suggested by Refsgaard and Storm (1996), ultimately leading to the final results. The optimized parameters are shown in Table 2.4.

3. RESULTS AND DISCUSSION

3.1. Modeling via the Original Anaerobic Digestion Model No.1's Parameters

Initially, the original ADM1 was implemented without any parameter optimization or modification to understand its behavior on anaerobic fermentation system operated at three different pH levels. In acidic condition (pH 5), while final total VFA concentration of experiment was 0.3 kg COD/m^3, final total VFA concentration of model simulation was 1.17 kg COD/m^3 (Figure 3.1). In control condition (pH 7), while final total VFA concentration of experiment was 0.032 kg COD/m^3, final total VFA concentration of model simulation was 0.25 kg COD/m^3 (Figure 3.1). In other words, total volatile fatty acid (VFA) concentration results of ADM1 for acidic and control conditions were extremely higher than experimental total VFA results (Figure3.1). This suggests that relatively higher hydrolysis rates *(k_{hyd})* of ADM1, compared to modified parameters of this study (Table 2.4), most likely resulted in higher total VFA concentrations during model simulations than the experimental total VFA concentrations.

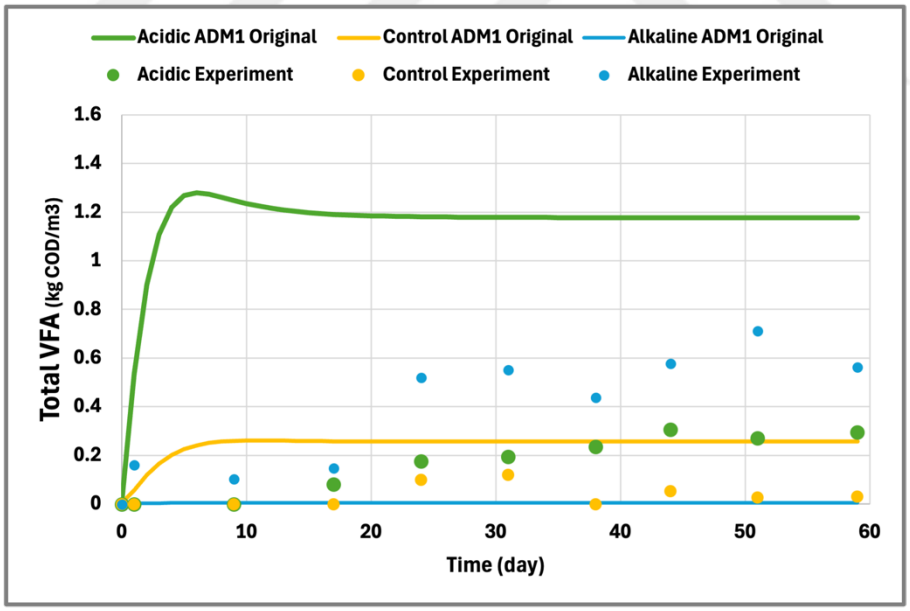

Figure 3.1. Total VFA concentration simulations of original ADM1, without any modification

In alkaline condition (pH 10), while final total VFA concentration of experiment was 0.56 kg COD/m^3, final total VFA concentration of model simulation was nearly zero (Figure 3.1). The main reason was the original ADM1 predicted that acidogenesis was blocked

by higher pH level (pH 10) and it resulted in lower total VFA concentrations than total VFA concentration results of experiment. As shown in Figure 3.1, ADM1 was insufficient for modeling anaerobic fermentation system operated with sewage sludge from an activated sludge system operated at solids retention time of approximately 20 days without any modification.

3.2. Model Results under Optimized Parameter Condition

Modified model was examined in terms of mass balance before comparing the results of experiment and model simulations (Appendix 2). This analysis demonstrated that the modified model codes had been applied correctly.

3.2.1. pH - free ammonia nitrogen (FAN)

In the experimental stage, Yesil et al. (2021b) have only controlled pH of the acidic and alkaline reactors through the addition of an acid or a base (Yesil et al., 2021b). Therefore, pH levels were set to 5 for acidic, 7 for control, and 10 for alkaline reactors (Figure 3.2)

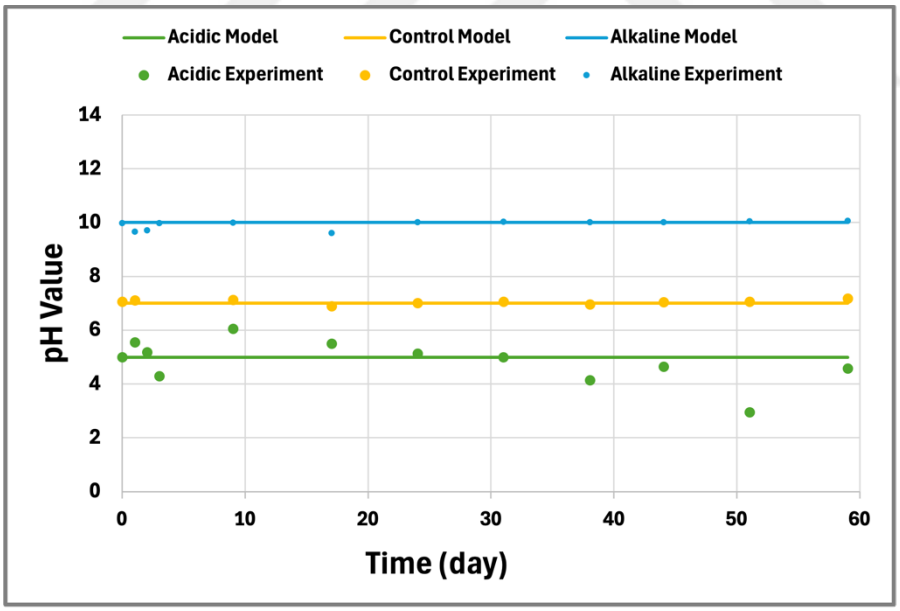

Figure 3.2. pH levels in the acidic, control (neutral), and alkaline reactors

During the non-treated feeding regime in acidic condition (pH 5), experimental free ammonia nitrogen (FAN) concentration rose up to 0.01 mg NH_3-N/L (Figure 3.3-b). In the same period, FAN concentration of model simulation increased from 0.008 to 0.01 mg NH_3-N/L (Figure 3.3-b). In pretreated feeding regime at acidic condition (pH 5),

experimental FAN concentration increased from 0.01 to 0.02 mg NH_3-N/L. In the same period at acidic condition (pH 5), FAN concentration of model simulation increased from 0.01 to 0.025 mg NH_3-N/L (Figure 3.3-b). It is clear that the correlation between experiment and model simulation results was rather successful in acidic condition for both feeding regime (Figure 3.3-b).

In control reactor (pH 7) without any pretreatment, FAN concentration increased from 1 mg NH_3-N/L to 1.3 mg NH_3-N/L (Figure 3.3-b). FAN concentration in the model simulation for the same period increased from 0.8 mg NH_3-N/L to 0.97 mg NH_3-N/L (Figure 3.3-b). After non-treated feeding regime at control condition, FAN concentration increased from 1.3 mg NH_3-N/L to 2.3 mg NH_3-N/L. In the same feeding regime and pH, the model simulation of FAN concentration increased from 0.97 mg NH_3-N/L to 2.45 mg NH_3-N/L (Figure 3.3-b). For control condition, and both feeding regime, acidic and control, modified ADM1 was well fitted to experimental results can be shown in Figure 3.3-b.

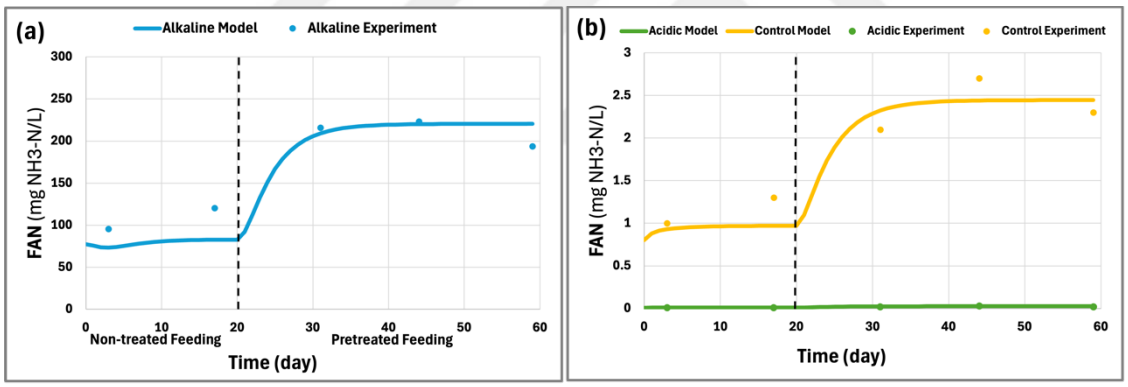

Figure 3.3. Free ammonia nitrogen concentration at pH 10 (a), pH 5, and pH 7 (b)

At pH 10 without any pretreatment, FAN concentration increased from 95 mg NH_3-N/L to 120 mg NH_3-N/L (Figure 3.3-a). Same period, model simulation results were slightly under the experimental results (Figure 3.3-a). After regime shifting in 20th day, FAN concentration rose up to 194 mg NH_3-N/L from 120 mg NH_3-N/L. In the model simulation for same period and pH, FAN concentration increased from 82 mg NH_3-N/L to 220 mg NH_3-N/L Figure 3.3-a. It can be easily seen from Figure 3.3-a that modified model was fitted to experimental results.

In summary, the pH level in the reactors was the most influential parameter affecting the FAN concentration. Because, physicochemical processes are significantly affect FAN

concentration in the reactors. In this study, experimental results at three different pH conditions were well simulated, including the pretreatment effect, with the developed model (Figure 3.3).

3.2.2. Disintegration and hydrolysis

The initial stages of anaerobic fermentation-digestion, disintegration and hydrolysis, take place in the extracellular environment. ADM1 uses first-order kinetics for disintegration and hydrolysis processes (Batstone et al., 2002). These relatively simple equations, purified from complexity, were chosen to align with ADM1's objective of simplicity. However, a long solid retention time (SRT) in sewage sludge leads to a significantly limited biodegradability and dewaterability, as its structure predominantly consists of composite material (Kianmehr et al., 2013; Lee, 1994; Zhang et al., 2017).

In general, the facility that uses activated sludge process are operated at SRT around 4-5 days (Tchobanoglous et al., 2014). In Yesil et al. (2021b)'s experiment, the SRT of facility where the sewage sludge-substrate taken was reported as 20 days by the plant operators, which shows that the plant was operated in an extended aeration mode. This suggested that the sludge-substrate taken had highly complex structure for disintegration and hydrolysis. Additionally, the SRT of the fermentation processes operated at three identical pH values (pH 5, pH 7, and pH 10) in three separate reactors in the experiment was only 4 days (Yesil et al., 2021b). The tightly bound composite structure of the sewage sludge, combined with the short SRT of the reactors, illustrates how challenging the hydrolysis step truly is.

In summary, sewage sludge with robust floc structure and a relatively short timeframe for pre-fermentation processes was used in the experiments. Therefore, the optimization of parameters began with the rate constants for disintegration *(k_{dis})* and hydrolysis *(k_{hyd})*.

3.2.2.1.Disintegration

The rate constants of disintegration of composite material *(k_{dis})* under both feeding regimes were presented in Table 2.4. These values were chosen rather similar to the original ADM1 parameters especially for non-treated feeding regime. Literature reviews report that acidic or alkaline conditions have a more pronounced positive effect on

disintegration compared to control conditions (Shi et al., 2022; Wang et al., 2017; Zawieja, 2019; Zhao et al., 2018). Given the known effects of alkaline and acidic conditions as pretreatment, the selected values were optimized considering the VFA results of the modeled experiment. Hence, a higher k_{dis} value was assigned, relative to the control condition for each pH level (Table 2.4). While the disintegration rate constants k_{dis} for the non-treated feeding regime were 0.6, 0.5, and 0.7 day^{-1} under acidic, control, and alkaline conditions, respectively, the disintegration rate constants for the pretreated feeding regime were 0.7, 0.7, and 0.8 day^{-1}.

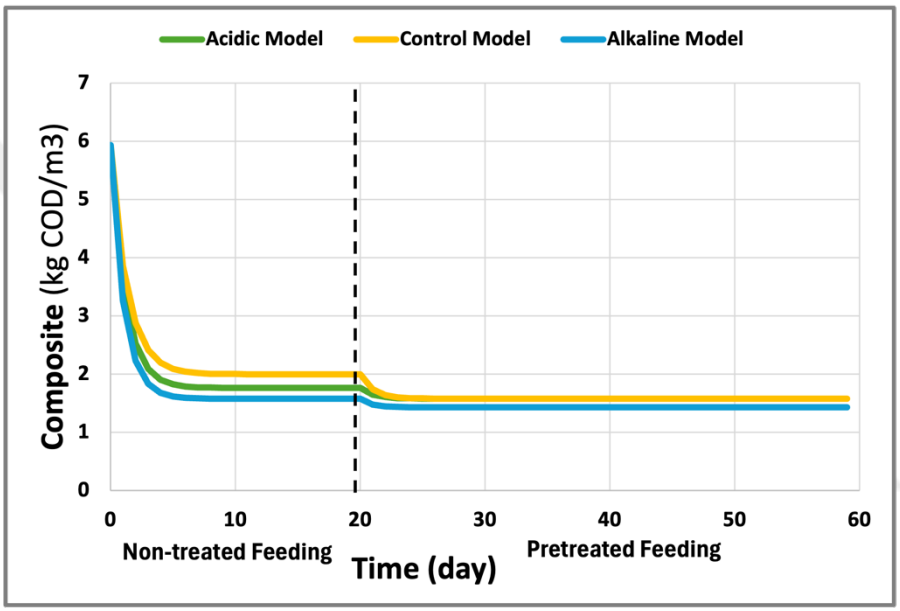

Figure 3.4. Model behavior during disintegration of composite material

Among the commonly used pretreatment methods is ultrasonication. This method relies on ultrasonic waves to break down the composite structure, and its positive contribution to disintegration has been studied in a number of studies (Aldin et al., 2010; Lizama et al., 2017; Negral et al., 2015; Passos et al., 2014; Zhen et al., 2017). Based on these findings, higher k_{dis} values were determined for the ultrasonicated substrate regime under all three pH conditions (Table 2.4). During the first 8 days, a rapid composite breakdown was observed, and the composite material decreased from 5.93 to 2.00, 1.76, and 1.58 kg COD/m^3 for the control, acidic, and alkaline conditions, respectively. Subsequently, as shown in Figure 3.4, the concentration of composite material remained stable until day 20th. After pretreatment, concentrations of composite material (X_c) decreased to 1.58, 1.57, and 1.42 kg COD/m^3 for the control, acidic, and alkaline conditions, respectively.

Prior to pretreatment, 70% reduction in the concentration of composite material was observed for all the pH controlled reactors (Figure 3.4). After pretreatment, despite the increase in kinetic rate constant *(k_{dis})* of three identical pH condition, the reduction in the composite materials *(X_c)* averaged around 6.2% (Figure 3.4). This was attributed to high inert composition of composite material in general as the sewage sludge generated in an activated sludge unit operated at long SRTs (20 days) was used as a feed.

The model simulation results for carbohydrate *(X_{ch})*, protein *(X_{pro})*, and lipid *(X_{li})* concentration, as illustrated in Figures 3.5-a, 3.6-a, and 3.7-a, clearly indicated that the transformation of the composite material into carbohydrates, proteins, and lipids due to degradation occurs during the first eight days. Under alkaline conditions, although the composite material concentration decreases more significantly compared to acidic and control conditions (Figure 3.4), the concentrations of carbohydrates, proteins, and lipids increased less than in acidic and control conditions (Figures 3.5a, 3.6a, and 3.7a). The composite disintegration rate constant *(k_{dis})*, which determines the degradation rate of the composite material in first-order kinetic equations, were 0.6, 0.5, and 0.7 d^{-1} for acidic, control, and alkaline conditions, respectively, under the non-treated feeding regime. The primary reason for this phenomenon is the rapid hydrolysis rate constants under alkaline conditions (Table 2.4). As the subsequent stage progresses rapidly, carbohydrates, proteins, and lipids undergo hydrolysis before accumulating in the model simulation.

3.2.2.2.Hydrolysis

The disintegration and hydrolysis processes of composite material, as described in Section 3.2.2, may proceed slowly depending on the sludge age, its composition, and other characteristic properties. Considering these factors and the performance of the original ADM1 on the experiment modeled as illustrated in Figure 3.1, the hydrolysis parameters for all three pH conditions in the modeled experiment were optimized as shown in Table 2.4. The optimization process began with lower hydrolysis rate constants *(k_{hyd})* such as 0.012 day^{-1} for non-treated feeding regime for control condition than the original ADM1 value of 10 day^{-1}, as explained in the previous sections. The initially identified broad ranges were narrowed and fine-tuned through trial and error, eventually reaching final values.

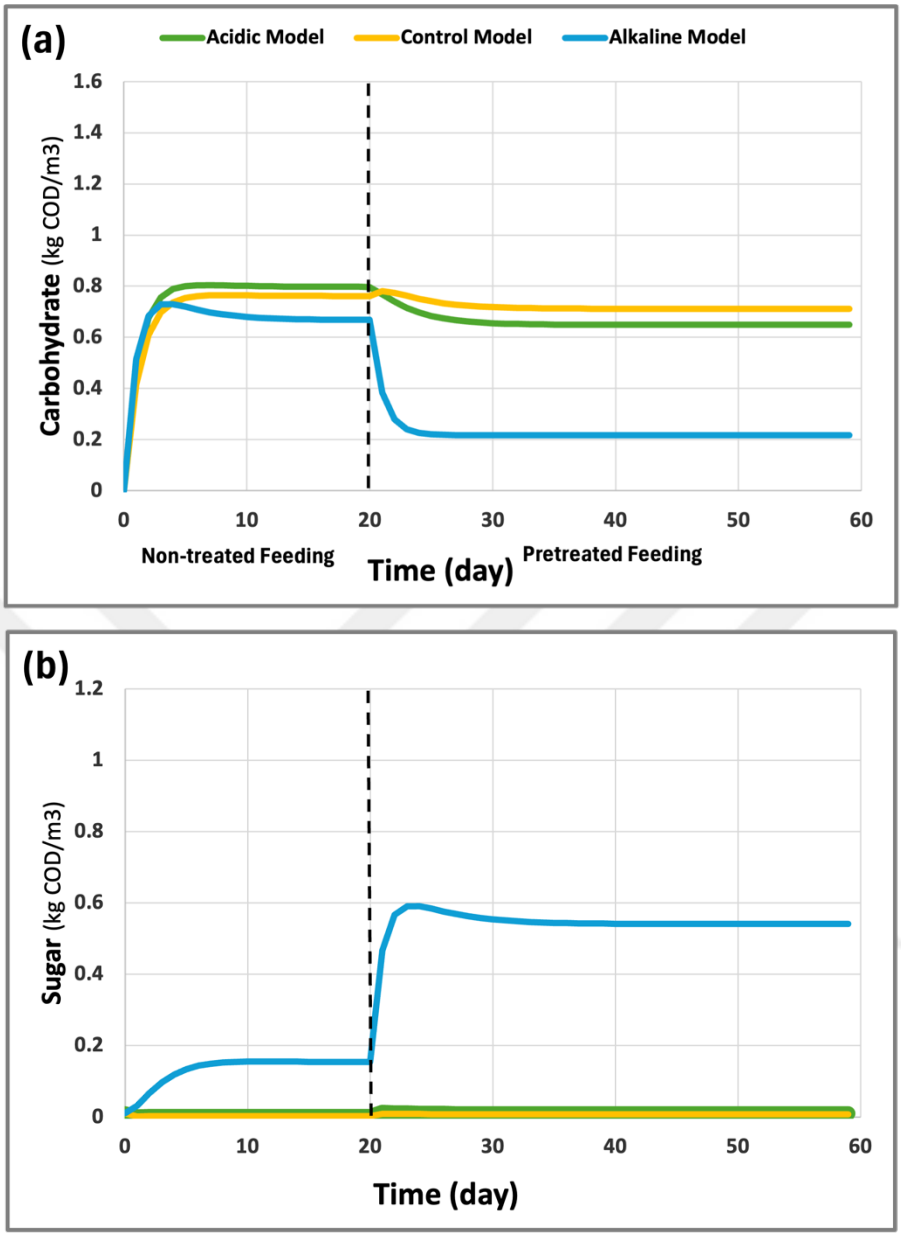

Figure 3.5. Fate of carbohydrate (a), and sugar (b) modeled via modified ADM1

For both feeding regimes (non-pretreated and pretreated) in the three reactors, the *(k_{hyd})* values determined were higher than those of the control condition, given the known positive effects of acidic and alkaline conditions on hydrolysis (Table 2.4) (Chen et al., 2007; Garcia-Aguirre et al., 2017; Li et al., 2017; Liu et al., 2012; Liu et al., 2014; Mengmeng et al., 2009; Wu et al., 2017; Zhou et al., 2021). Additionally, under all three pH conditions, hydrolysis rate constants *(k_{hyd})* were set higher for the pretreated feeding regime compared to the non-treated one (Lizama et al., 2017; Passos et al., 2014; Zerrouki et al., 2021), with the effect being more pronounced under alkaline conditions (Table 2.4).

Upon examining the optimized parameters, it was clearly observed that higher hydrolysis rates were achieved under alkaline conditions compared to acidic conditions. This suggests that the increased FAN, along with the rising pH, also contributes to the acceleration of the hydrolysis rate. In other words, a synergistic effect of pH and FAN on hydrolysis was observed.

When the hydrolysis simulation results were examined, it was observed that under acidic and control conditions without pretreatment, there is no significant decrease after peak points (after 4th days of acidic and control condition) in the concentrations of carbohydrates, proteins, and lipids within the first 20 days. However, under the alkaline condition without pretreatment, carbohydrate, protein, and lipid concentrations decrease from their peaks (after 4th day of alkaline condition) by almost 9%, (Figure 3.5-a, Figure 3.6-a, Figure 3.7-a). Consequently, under the alkaline condition without pretreatment, the concentration of sugars, amino acids, and long chain fatty acids (LCFAs) increase to 0.15, 0.081, and 0.30 kg COD/m^3, respectively (Figure 3.5-b, Figure 3.6-b, Figure 3.7-b). Concentrations of carbohydrates, proteins and lipids in alkaline condition without pretreatment decrease by the same rate (9%) (Figure 3.5-a, Figure 3.6-a, Figure 3.7-a), the reason why sugar, amino acid, and lipid concentrations did not increase at the same rate (Figure 3.5-b, Figure 3.6-b, Figure 3.7-b) can be attributed to differences in acidification rates of sugars, amino acids, and lipids.

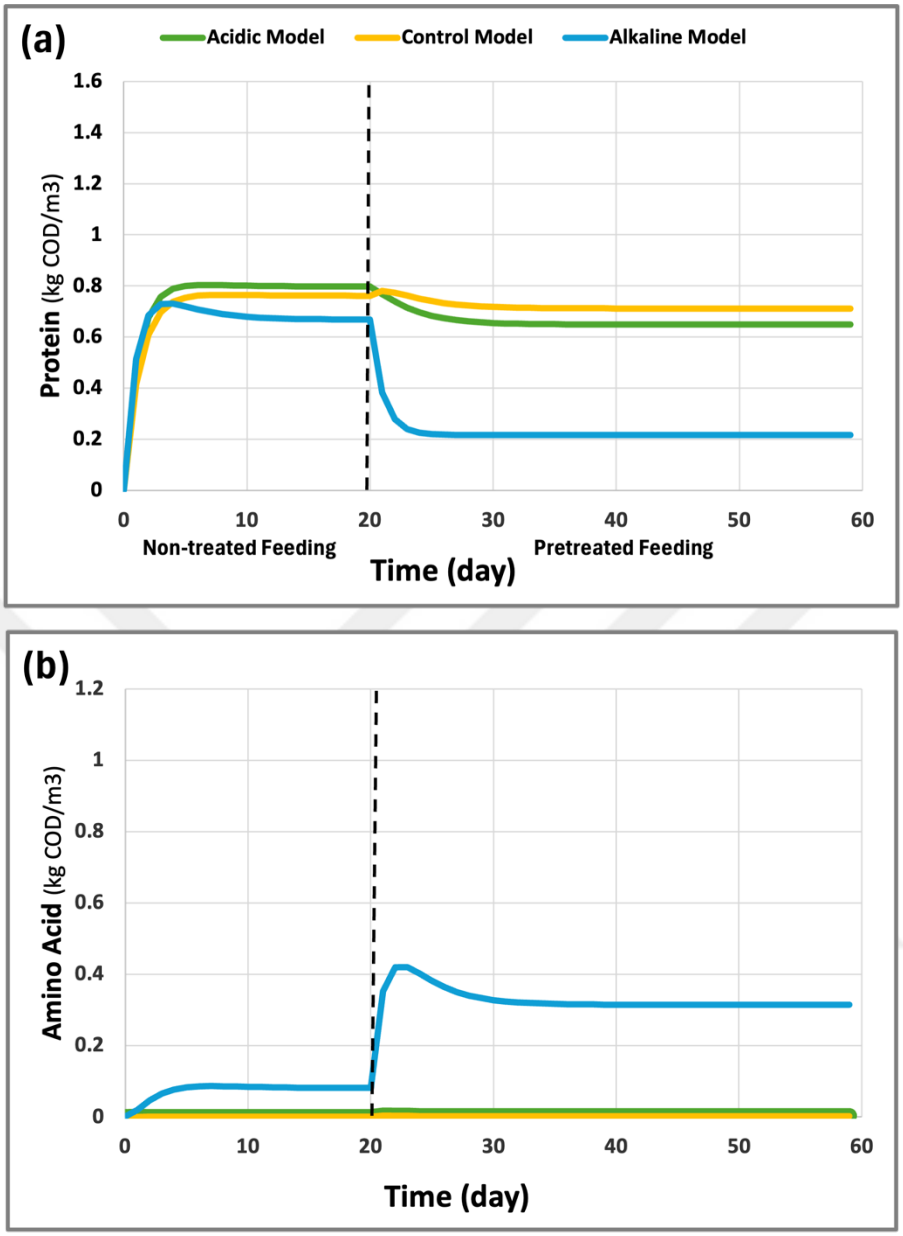

Figure 3.6. Fate of protein (a), and amino acid (b) modeled via modified ADM1

After the 20th day of the model simulation, under the pretreated feeding regime at all pH conditions, a decrease in the concentrations of carbohydrates, proteins, or lipids was observed (Figure 3.5-a, Figure 3.6-a, Figure 3.7-a). However, under control conditions, the concentrations of these components exhibit a slight increase at 22nd day followed by a decrease, which differs from the acidic and alkaline conditions, as shown in the graphs (Figure 3.5-a, Figure 3.6-a, Figure 3.7-a). This fluctuation observed under control conditions can be explained by the slower hydrolysis rate in this settings comparing with acidic, and alkaline conditions. In other words, the amount of carbohydrates, proteins,

and lipids generated by disintegration temporarily exceeds the amount reduced through hydrolysis of these molecules at pH 7 under pretreated feeding.

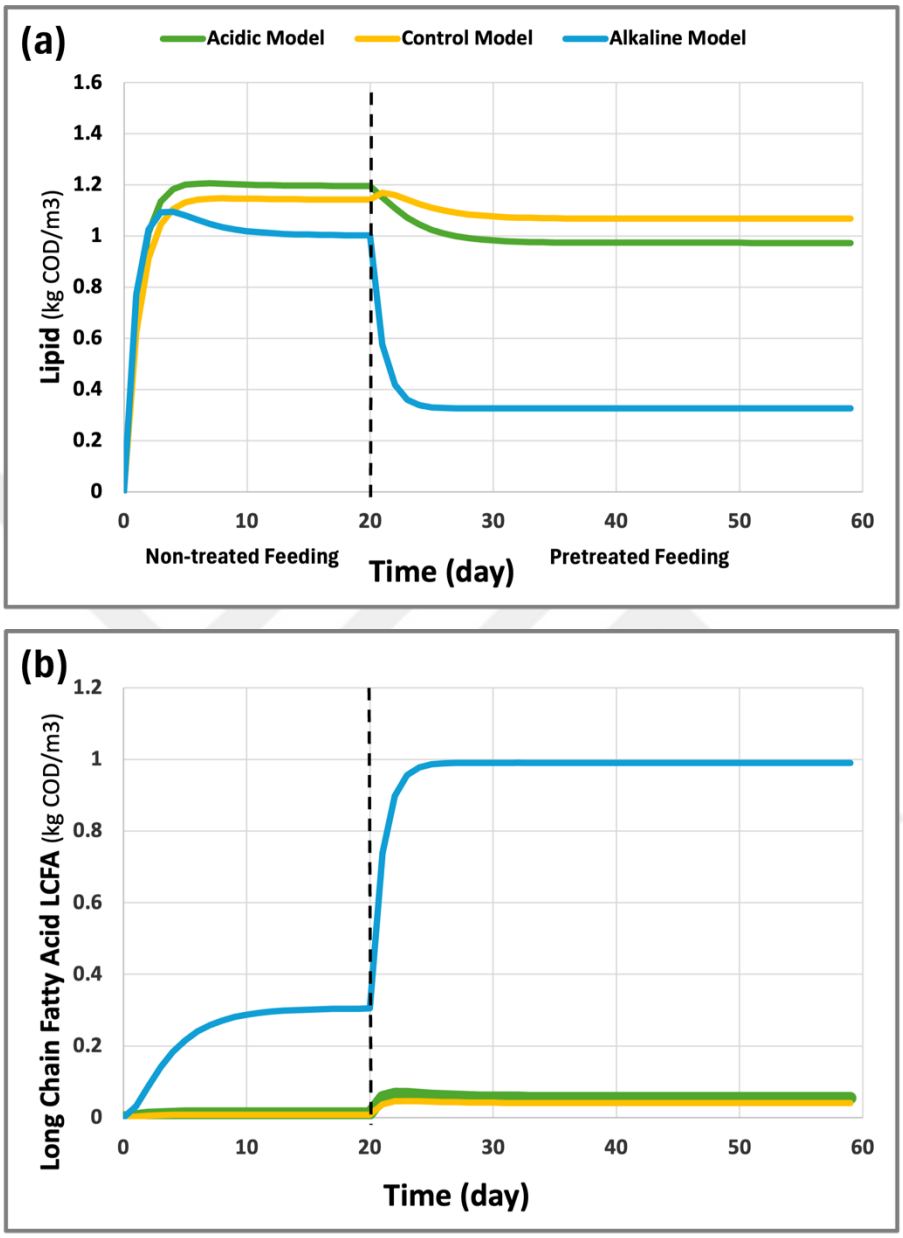

Figure 3.7. Fate of lipid (a), and long chain fatty acid (LCFA) (b) modeled via modified ADM1

In the pretreated feeding regime, the concentrations of carbohydrates, proteins, and lipids decreased from their peaks (20th-22nd days) by 19%, 19%, and 19% under acidic conditions; by 5%, 7%, and 6% under control conditions; and by 67%, 67%, and 67% under alkaline conditions, respectively (Figure 3.5-a, Figure 3.6-a, Figure 3.7-a). Correspondingly, the concentrations of sugars, amino acids, and LCFAs increased to 0.01,

0.004, and 0.06 kg COD/m^3 under acidic conditions; to 0.007, 0.003, and 0.04 kg COD/m^3 under control conditions; and to 0.54, 0.32, and 0.99 kg COD/m^3 under alkaline conditions, respectively (Figure 3.5-b, Figure 3.6-b, Figure 3.7-b). It can be easily understood that when the hydrolysis of carbohydrates, proteins, and lipids was examined, it was found to be consistent with the generation of sugars, amino acids, and long-chain fatty acids (LCFAs).

When the subsequent two different feeding regime for all pH condition simulations are evaluated, the positive impact of pretreatment on hydrolysis and consequently on VFA production has been clearly reflected in the model through parameter optimization. It is clear that there is a significant increase in hydrolysis rate in the pretreated regime compared to the first 20 days. The observation that the most substantial concentration increase occurs in LCFAs in both regimes is consistent with the lipid fraction of composite *($f_{li,Xc}$:0.3)* initially determined (Table 2.1).

3.2.3. Fermentation

In the previous section, the changes in the concentrations of carbohydrates, proteins, and lipids under acidic, control, and alkaline conditions during the hydrolysis stage of the model simulation were examined, and the resulting concentrations of sugar, protein, and lipid molecules were shared. In this section, changes in sugar, protein, and lipid molecules undergoing acidification with a focus on VFA concentrations were analyzed.

When the simulation results of the non-treated feeding regime were examined, a significant increase in the concentrations of sugars, amino acids, and LCFAs were observed only under alkaline condition (Figure 3.5-b, Figure 3.6-b, Figure 3.7-b). However, no significant decrease in the concentrations of sugars, amino acids, and LCFAs after their peak values was detected for all pH conditions in non-treated feeding regime (Figure 3.5-b, Figure 3.6-b, Figure 3.7-b). This was consistent with the low total VFA concentration of experiment observed up to the 20th day (Figure 3.8). In the pretreated feeding regime under alkaline conditions, sugar and amino acid concentrations decreased by 9% and 20%, respectively, from their peak values (22nd day) (Figure 3.5-b, Figure 3.6-b). Under acidic and control conditions, despite the pretreatment, the decreases in sugar, amino acid, and LCFA concentrations from their peak values (22nd day) remained minimum, similar to the non-treated feeding regime period (Figure 3.5-b, Figure 3.6-b,

Figure 3.7-b). Hence, it can be inferred that especially under the alkaline condition, VFAs are predominantly formed from the fermentation of sugars and amino acids.

On the 17th day, non-treated feeding regime in the experiment, the total VFA concentrations reached 0.082, 0, and 0.15 kg COD/m^3 for acidic, control, and alkaline conditions (pH 5, pH 7, pH 10), respectively (Figure 3.8). On the final day of the pretreated feeding regime of experiment, which is the 59th day, the total VFA concentrations reached 0.295, 0.032, and 0.563 kg COD/m^3 for acidic, control and alkaline conditions (Figure 3.8). On the 20th day of model simulation, the total VFA concentrations increased to 0.042, 0.007, and 0.18 kg COD/m^3 for acidic, control, and alkaline conditions, respectively (Figure 3.8). On the final day of the model simulations under the pretreated feeding regime, which is the 59th day, the total VFA concentrations reached 0.24, 0.032, and 0.49 kg COD/m^3 in the same order. In all feeding regimes, there was no significant decrease in concentrations of total VFA after the peak points (10th and 25th day for acidic, 3rd and 22nd for control, 18th and 40th for alkaline condition), except under acidic conditions (Figure 3.8). In other words, except for the minimal conversion observed under acidic conditions, VFAs have not been converted into gas during model simulations.

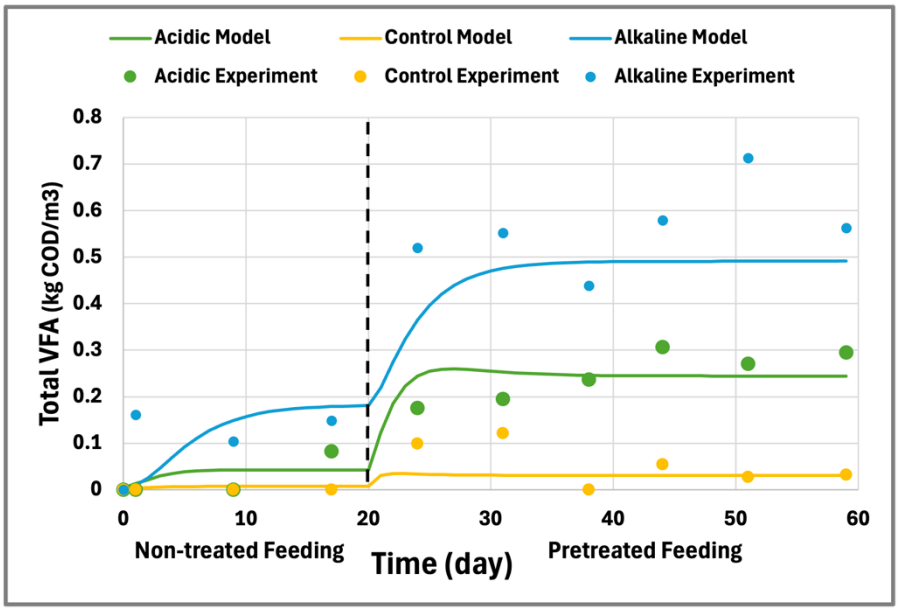

Figure 3.8. Fate of total VFAs modeled via modified ADM1

Modified ADM1 was well fitted to experimental results. Positive effect of pretreatment to total VFA producing capacity was well integrated to the ADM1 to be able to simulate

can be seen in the Figure 3.8 on 20th day. As given in the previous paragraph, the simulation of total VFA concentration reached its highest level under alkaline conditions (Figure 3.8).

In section 3.1, ADM1's total VFA model simulation results had been examined via comparing the Yesil et al. (2021b)'s experimental total VFA results. It was clear that the gap between ADM1 total VFA simulation results and experimental total VFA concentration results were extremely unequal (Figure 3.1). Fortunately, while modified model was able to lower ADM1's relatively higher total VFA concentration estimations under acidic and control condition, it was able to higher ADM1's nearly zero total VFA concentration estimations by fitting well with experimental total VFA results in alkaline condition (Figure 3.8).

Prior to analyzing the model results of individual volatile fatty acids (VFAs), it would be beneficial to focus on the optimized parameters (Table 2.4). Although model simulations performed after optimizing the disintegration and hydrolysis values showed complete agreement for total VFA values (Figure 3.8), imbalances were observed in individual VFAs, particularly under acidic and alkaline conditions. To address these imbalances, a literature review was conducted, focusing on fermentation studies under acidic and alkaline conditions (Garcia-Aguirre et al., 2017; Huang et al., 2018; Li et al., 2017; Liu et al., 2012; Regueira et al., 2021; Shi et al., 2022; Wu et al., 2017; Yu et al., 2008). For acidic conditions, there were studies showing not only the time-dependent changes in total VFA concentrations but also changes in the ratios of individual VFAs (Garcia-Aguirre et al., 2017; Huang et al., 2018; Liu et al., 2012; Regueira et al., 2021; Shi et al., 2022). Based on these, the parameters $k_{m,pro}$, $k_{s,pro}$, $k_{m,c4}$, and $k_{s,c4}$ were optimized and fine-tuned through trial and error approach for acidic condition ($k_{m,pro}$, $k_{s,pro}$, $k_{m,c4}$, and $k_{s,c4}$ were calibrated to 4, 0.3, 7, 0.6 day^{-1}) (Table 2.4) . In alkaline conditions, there were studies showing the stoichiometric distribution of amino acids during fermentation can differ (Li et al., 2017; Liu et al., 2012; Liu et al., 2014; Regueira et al., 2021). Using the stoichiometric coefficients from the study conducted by Liu et al. (2012) (details in Appendix 1), the necessary calculations were performed for alkaline condition (Table 2.3). The final stoichiometric fractions obtained from these calculations were previously presented in Table 2.3 in Section 2.3.1.2.

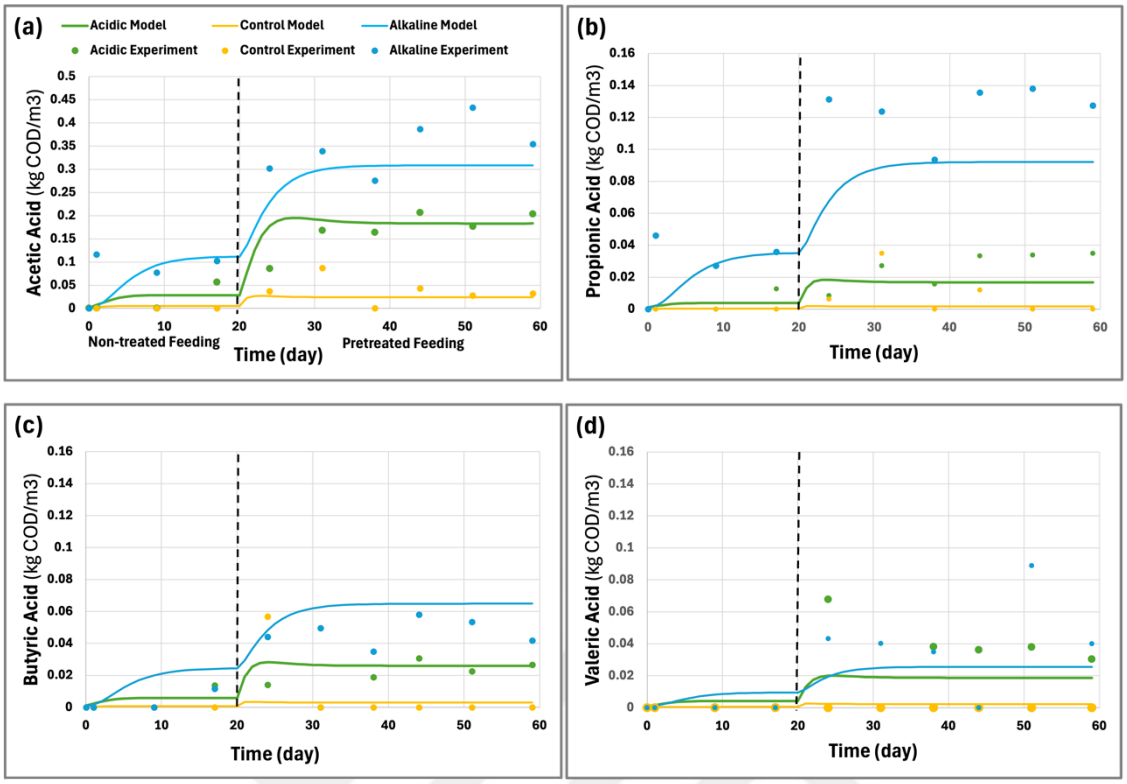

Figure 3.9. Fate of acetic acid (a), propionic acid (b), butyric acid (c), and valeric acid (d) modeled via modified ADM1

Figure 3.9 shows the time-dependent changes in the simulation and experimental concentration results of acetic, propionic, butyric, and valeric acids. Upon detailed examination, it was clearly observed that the change trends in the graphs were consistent. Among the three pH conditions, the most consistent one was the graph showing the time-dependent change in acetic acid concentration (Figure 3.9-a).

When examined the distribution of composite *(X_c)* in anaerobic fermentation-digestion (Figure 1.5) (Batstone et al., 2002), it was easily understood that a portion of propionic, butyric, and valeric acids were also converted into acetate. Consistent with this, the proportion of acetic acid in the total VFA concentration under acidic, control, and alkaline conditions was 75%, 76%, and 61%, respectively (Figure 3.8, Figure 3.9-a). This situation explains why the total VFA concentration predictions for all pH levels (pH 5, pH 7, pH 10) were well fitted to experimental results (Figure 3.8), despite the imperfect predictions for butyric valeric acids (Figure 3.9-c, Figure 3.9-d).

The experimental data by Yesil et al. (2021b) were given in Section 2.1. Since initial organic loading rates (OLRs) of the reactors operating under different pH conditions

(pH5, pH 7, pH 10) was low (OLR: 1.17 kg VS/m^3·d), the measured VFAs in the experiment were also at quite minor values (Figure 3.9). Considering the difficulty of measuring such sensitive values, it can be stated that the model simulation results for all pH levels were relatively good, even for the concentration of butyric and valeric acids (Figure 3.9-c, Figure 3.9-d).

3.3. Validation

The validation of a modeled anaerobic fermentation process with different data sets will provide confidence to the user regarding the usability of this model for simulating any fermentation system (Batstone et al., 2002; Batstone et al., 2015). In this context, the model developed for alkaline conditions was validated using the experiment described in Section 2.2 (Yeşil, 2021). The optimized parameters for alkaline condition (pH 10)(Table 2.4) without pretreatment were used during validation process in order to observe the modified model behavior under different anaerobic fermentation system (Yeşil, 2021). Furthermore, modified model simulation results (y axis of Figure 3.10-b), and experimental results (x axis of Figure 3.10-b) were compared via R^2 method (Mevik & Wehrens, 2007). While Total VFA concentration of experiment increased from 0.04 to 6.2 kg COD/m^3, the concentration of total VFA of model simulation increased from 0.04 to 5.07 kg COD/m^3 (Figure 3.10-a). Notably, a quite good trend was observed between the model simulation and experimental results, especially during the first 10 days and after the 30th day of the operated reactor (Figure 3.10-a).

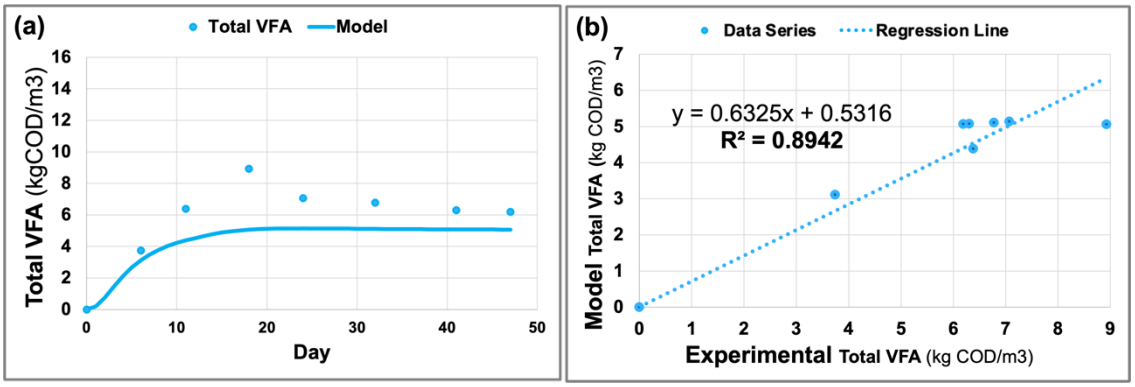

Figure 3.10. Total VFA concentration comparison between experiment and model (a), and R^2 value of model (b)

In Figure 3.10-b, where the total VFA concentrations are compared, the experimental data on the x-axis and the model results on the y-axis, the R^2 value was determined to be 0.89 which demonstrated the capability of modified model for a particular fermentation system (Yeşil, 2021).

4. CONCLUSIONS

In this study, the ADM1 was modified via optimized parameters such as disintegration *(k_{dis})*, hydrolysis *(k_{hyd})*, and volatile fatty acid (VFA) utilization rates *(k_{mpro}, k_{spro}, k_{mc4}, k_{sc4})* (Table 2.4). In addition to that, stoichiometric coefficients of amino acids *($f_{ac,aa}$, $f_{pro,aa}$, $f_{bu,aa}$, $f_{va,aa}$ $f_{h2,aa}$)* were calculated (Appendix 1) in line with Liu et al. (2012) for alkaline condition (pH 10) (Table 2.3). Hence, the modified ADM1 were able to successfully simulate the anaerobic fermentation systems operated under identical pH conditions (pH 5, pH 7, pH 10) fed with both non-treated and pretreated sewage sludge (Yeşil, 2021) (Figure 3.8, Figure 3.9).

The key findings of this thesis include:

- Free ammonia nitrogen (FAN) and total VFA concentrations of all pH conditions (pH 5, pH 7, and pH 10) were successfully modeled including the pretreatment effect of ultrasonication (Figure 3.3, Figure 3.8).
- Individual VFAs as acetic, propionic, butyric, and valeric acid concentrations were well estimated especially under alkaline condition including pretreatment effect of ultrasonication (Figure 3.9).
- The modified model validated for examining the consistency of experimental data and the model simulation. Thus, model depicted the distinct dynamics of fermentation processes at varying pH levels (pH 9), achieving a strong correlation between experimental and simulation results under alkaline condition (R^2= 0.89 for total volatile fatty acids) (Figure 3.10).
- Systematic optimization of parameters, including stoichiometric coefficients and rate constants, ensured accurate modeling of the complex interactions within the fermentation system, despite the challenges posed by sensitive measurements and low organic loading rates (OLRs) such as 1.17 kg VS/m^3.d.

These findings emphasize the potential of modeling of anaerobic fermentation systems pretreated with ultrasonication under varied pH conditions. The modified ADM1 offers a robust framework for simulating similar systems, paving the way for future studies that explore the synergistic effects of pretreatment methods and variable pH conditions. Besides, given the increasing importance of VFA recovery, the ability to estimate VFA

concentrations through modeling with the modified ADM1 will become even more valuable in the near future.

Further research is recommended to validate the model across a broader range of operational conditions and substrates. Characterization of the particulate organic matter is required to determine all the stoichiometric parameters used in the model. Additionally, integrating the modified ADM1 into industrial-scale applications could provide valuable insights into its scalability and economic feasibility, contributing to the advancement of circular economy principles in wastewater management.

REFERENCES

Adar, E., Karatop, B., İnce, M., & Bilgili, M. S. (2016). Comparison of methods for sustainable energy management with sewage sludge in Turkey based on SWOT-FAHP analysis. *Renewable and Sustainable Energy Reviews*, *62*, 429-440. https://doi.org/10.1016/j.rser.2016.05.007

Adhikari, R. (2006). Sequential batch and continuous anaerobic digestion of municipal solid waste in pilot scale digesters. *Master of Science, School of Environment, Resources and Development, Asian Institute of technology, Thailand*.

Agler, M. T., Wrenn, B. A., Zinder, S. H., & Angenent, L. T. (2011). Waste to bioproduct conversion with undefined mixed cultures: the carboxylate platform. *Trends in Biotechnology*, *29*(2), 70-78. https://doi.org/10.1016/j.tibtech.2010.11.006

Agnihotri, S., Yin, D.-M., Mahboubi, A., Sapmaz, T., Varjani, S., Qiao, W., Koseoglu-Imer, D. Y., & Taherzadeh, M. J. (2022). A Glimpse of the World of Volatile Fatty Acids Production and Application: A review. *Bioengineered*, *13*(1), 1249-1275. https://doi.org/10.1080/21655979.2021.1996044

Agnihotri, S., Yin, D. M., Mahboubi, A., Sapmaz, T., Varjani, S., Qiao, W., Koseoglu-Imer, D. Y., & Taherzadeh, M. J. (2022). A Glimpse of the World of Volatile Fatty Acids Production and Application: A review. *Bioengineered*, *13*(1), 1249-1275. https://doi.org/10.1080/21655979.2021.1996044

Aldin, S., Elbeshbishy, E., Nakhla, G., & Ray, M. B. (2010). Modeling the Effect of Sonication on the Anaerobic Digestion of Biosolids. *Energy & Fuels*, *24*(9), 4703-4711. https://doi.org/10.1021/ef901255k

Ariunbaatar, J., Panico, A., Esposito, G., Pirozzi, F., & Lens, P. N. L. (2014). Pretreatment methods to enhance anaerobic digestion of organic solid waste. *Applied Energy*, *123*, 143-156. https://doi.org/https://doi.org/10.1016/j.apenergy.2014.02.035

Bai, J., Liu, H., Yin, B., & Ma, H. (2015). Modeling of enhanced VFAs production from waste activated sludge by modified ADM1 with improved particle swarm optimization for parameters estimation. *Biochemical Engineering Journal*, *103*, 22-31. https://doi.org/https://doi.org/10.1016/j.bej.2015.06.015

Bai, J., Liu, H., Yin, B., Ma, H., & Chen, X. (2017). Modified ADM1 for modeling free ammonia inhibition in anaerobic acidogenic fermentation with high-solid sludge. *Journal of Environmental Sciences*, *52*, 58-65. https://doi.org/https://doi.org/10.1016/j.jes.2016.03.004

Baird, C., & Cann, M. (2012). *Environmental chemistry* (5th edition ed.). W.H. Freeman and Company.

Batstone, D. (2006). Mathematical Modelling of Anaerobic Reactors Treating Domestic Wastewater: Rational Criteria for Model Use. *Reviews in Environmental Science and Bio/Technology*, *5*. https://doi.org/10.1007/s11157-005-7191-z

Batstone, D., Keller, J., Angelidaki, I., Kalyuzhnyi, S., Pavlostathis, S., Rozzi, A., Sanders, W., Siegrist, H., & Vavilin, V. (2002). Anaerobic digestion model No 1 (ADM1). *Water science and technology : a journal of the International Association on Water Pollution Research*, *45*, 65-73.

Batstone, D., Keller, J., & Steyer, J. P. (2006). A review of ADM1 extensions, applications, and analysis: 2002-2005. *Water science and technology : a journal of the International Association on Water Pollution Research*, *54*, 1-10. https://doi.org/10.2166/wst.2006.520

Batstone, D. J., Puyol, D., Flores-Alsina, X., & Rodríguez, J. (2015). Mathematical modelling of anaerobic digestion processes: applications and future needs. *Reviews in Environmental Science and Bio/Technology*, *14*(4), 595-613. https://doi.org/10.1007/s11157-015-9376-4

Batstone, D. J., & Rodríguez, J. (2015). Modelling Anaerobic Digestion Processes. In *Anaerobic Biotechnology* (pp. 133-160). https://doi.org/10.1142/9781783267910_0007

Batstone, D. J., Tait, S., & Starrenburg, D. (2009). Estimation of hydrolysis parameters in full-scale anerobic digesters. *Biotechnology and Bioengineering*, *102*(5), 1513-1520. https://doi.org/https://doi.org/10.1002/bit.22163

Bedaso, B. (2019). Volatile fatty acid production from co-fermentation of primary sludge and food waste without pH control. In.

Bochmann, G., & Montgomery, L. F. R. (2013). 4 - Storage and pre-treatment of substrates for biogas production. In A. Wellinger, J. Murphy, & D. Baxter (Eds.), *The*

Biogas Handbook (pp. 85-103). Woodhead Publishing. https://doi.org/https://doi.org/10.1533/9780857097415.1.85

Bougrier, C., Carrère, H., & Delgenès, J. P. (2005). Solubilisation of waste-activated sludge by ultrasonic treatment. *Chemical Engineering Journal*, *106*(2), 163-169. https://doi.org/https://doi.org/10.1016/j.cej.2004.11.013

Briard, M., O' Brien, S., & Pelsy, F. (2018). *A European strategy for plastics in the circular economy local and regional dimension*. European Committee of the Regions. https://doi.org/doi/10.2863/734820

Buruiana, D. L., Lefter, D., Tiron, G. L., Balta, S., Bordei, M., & Sgem. (2015, Jun 18-24). TOXICITY OF HEAVY METALS ON THE ENVIRONMENT AND HUMAN HEALTH.*International Multidisciplinary Scientific GeoConference-SGEM* [Ecology, economics, education and legislation, vol ii]. 15th International Multidisciplinary Scientific Geoconference (SGEM), Albena, BULGARIA.

Cao, Y., & Pawłowski, A. (2012). Sewage sludge-to-energy approaches based on anaerobic digestion and pyrolysis: Brief overview and energy efficiency assessment. *Renewable and Sustainable Energy Reviews*, *16*(3), 1657-1665. https://doi.org/https://doi.org/10.1016/j.rser.2011.12.014

Chang, Z., Long, G., Zhou, J. L., & Ma, C. (2020). Valorization of sewage sludge in the fabrication of construction and building materials: A review. *Resources, Conservation and Recycling*, *154*, 104606. https://doi.org/https://doi.org/10.1016/j.resconrec.2019.104606

Chen, Y., Jiang, S., Yuan, H., Zhou, Q., & Gu, G. (2007). Hydrolysis and acidification of waste activated sludge at different pHs. *Water Research*, *41*(3), 683-689. https://doi.org/https://doi.org/10.1016/j.watres.2006.07.030

Choudhury, A., Shelford, T., Felton, G., Gooch, C., & Lansing, S. (2019). Evaluation of Hydrogen Sulfide Scrubbing Systems for Anaerobic Digesters on Two U.S. Dairy Farms. *Energies*, *12*(24), 4605. https://www.mdpi.com/1996-1073/12/24/4605

Demirbas, A., Edris, G., & Alalayah, W. M. (2017). Sludge production from municipal wastewater treatment in sewage treatment plant. *Energy Sources, Part A: Recovery, Utilization, and Environmental Effects*, *39*(10), 999-1006.

EPA. (1993). *40 CFR Part 503*. https://www.ecfr.gov/current/title-40/part-503

EPA. (2005). *Examples of Equivalent Processes: PFRP and PSRP*. https://www.epa.gov/biosolids/examples-equivalent-processes-pfrp-and-psrp#PFRP

Eurostat. (2024). *Sewage sludge production and disposal from urban wastewater*. EuroStat. https://ec.europa.eu/eurostat/databrowser/view/ten00030/default/table?lang=en

Fang, H. H. P. (2015). *Anaerobic Biotechnology: Environmental Protection and Resource Recovery*. Imperial College Press. https://books.google.com.tr/books?id=efMZjwEACAAJ

Franke-Whittle, I. H., Walter, A., Ebner, C., & Insam, H. (2014). Investigation into the effect of high concentrations of volatile fatty acids in anaerobic digestion on methanogenic communities. *Waste Manag*, *34*(11), 2080-2089. https://doi.org/10.1016/j.wasman.2014.07.020

Garcia-Aguirre, J., Aymerich, E., González-Mtnez. de Goñi, J., & Esteban-Gutiérrez, M. (2017). Selective VFA production potential from organic waste streams: Assessing temperature and pH influence. *Bioresource Technology*, *244*, 1081-1088. https://doi.org/https://doi.org/10.1016/j.biortech.2017.07.187

Ghangrekar, M. M. (2022). Wastewater to Water.

González-Fernández, C., & García-Encina, P. A. (2009). Impact of substrate to inoculum ratio in anaerobic digestion of swine slurry. *Biomass and Bioenergy*, *33*(8), 1065-1069. https://doi.org/https://doi.org/10.1016/j.biombioe.2009.03.008

Harikishan, S. (2008a). Biogas Processing and Utilization as an Energy Source. In *Anaerobic Biotechnology for Bioenergy Production* (pp. 267-291). https://doi.org/https://doi.org/10.1002/9780813804545.ch12

Harikishan, S. (2008b). Pretreatment of High-Solids Wastes/Residues to Enhance Bioenergy Recovery. In *Anaerobic Biotechnology for Bioenergy Production* (pp. 247-265). https://doi.org/https://doi.org/10.1002/9780813804545.ch11

Harrison, S. T. L. (1991). Bacterial cell disruption: A key unit operation in the recovery of intracellular products. *Biotechnology Advances*, *9*(2), 217-240. https://doi.org/https://doi.org/10.1016/0734-9750(91)90005-G

Hartmann, H., & Ahring, B. K. (2006). Strategies for the anaerobic digestion of the organic fraction of municipal solid waste: an overview. *Water Science and Technology*, *53*(8), 7-22. https://doi.org/10.2166/wst.2006.231

Huang, L., Pan, X.-R., Wang, Y.-Z., Li, C.-X., Chen, C.-B., Zhao, Q.-B., Mu, Y., Yu, H.-Q., & Li, W.-W. (2018). Modeling of acetate-type fermentation of sugar-containing wastewater under acidic pH conditions. *Bioresource Technology*, *248*, 148-155. https://doi.org/https://doi.org/10.1016/j.biortech.2017.06.071

Inglezakis, V. J., Zorpas, A. A., Karagiannidis, A., Samaras, P., Voukkali, I., & Sklari, S. (2014). European Union legislation on sewage sludge management. *Fresenius Environmental Bulletin*, *23*(2), 635-639.

Jiang, J., Zhang, Y., Li, K., Wang, Q., Gong, C., & Li, M. (2013). Volatile fatty acids production from food waste: Effects of pH, temperature, and organic loading rate. *Bioresource Technology*, *143*, 525-530. https://doi.org/https://doi.org/10.1016/j.biortech.2013.06.025

Khanal, S. K. (2008a). Anaerobic Reactor Configurations for Bioenergy Production. In *Anaerobic Biotechnology for Bioenergy Production* (pp. 93-114). https://doi.org/https://doi.org/10.1002/9780813804545.ch5

Khanal, S. K. (2008b). Bioenergy Generation from Residues of Biofuel Industries. In *Anaerobic Biotechnology for Bioenergy Production* (pp. 161-188). https://doi.org/https://doi.org/10.1002/9780813804545.ch8

Khanal, S. K. (2008c). Environmental Factors. In *Anaerobic Biotechnology for Bioenergy Production* (pp. 43-63). https://doi.org/https://doi.org/10.1002/9780813804545.ch3

Khanal, S. K. (2008d). Overview of Anaerobic Biotechnology. In *Anaerobic Biotechnology for Bioenergy Production* (pp. 1-27). https://doi.org/https://doi.org/10.1002/9780813804545.ch1

Kianmehr, P., Parker, W., & Seto, P. (2013). Assessment of Waste-Activated-Sludge Pretreatment by Ultrasound and Applicability of Biodegradability Indicators. *Journal of*

Environmental Engineering, *139*(4), 545-553. https://doi.org/doi:10.1061/(ASCE)EE.1943-7870.0000657

Kim, D.-H., Jeong, E., Oh, S.-E., & Shin, H.-S. (2010). Combined (alkaline+ultrasonic) pretreatment effect on sewage sludge disintegration. *Water Research*, *44*(10), 3093-3100. https://doi.org/https://doi.org/10.1016/j.watres.2010.02.032

Kiran, Bharti, R., & Sharma, R. (2022). Effect of heavy metals: An overview. *Materials Today: Proceedings*, *51*, 880-885. https://doi.org/https://doi.org/10.1016/j.matpr.2021.06.278

Kiselev, A., Magaril, E., Magaril, R., Panepinto, D., Ravina, M., & Zanetti, M. C. (2019). Towards Circular Economy: Evaluation of Sewage Sludge Biogas Solutions. *Resources*, *8*(2), 91. https://www.mdpi.com/2079-9276/8/2/91

Kumar, A. K., & Sharma, S. (2017). Recent updates on different methods of pretreatment of lignocellulosic feedstocks: a review. *Bioresour Bioprocess*, *4*(1), 7. https://doi.org/10.1186/s40643-017-0137-9

Kuttruff, H. (2012). *Ultrasonics: Fundamentals and applications*. Springer Science & Business Media.

Laiq Ur Rehman, M., Iqbal, A., Chang, C.-C., Li, W., & Ju, M. (2019). Anaerobic digestion. *Water Environment Research*, *91*(10), 1253-1271. https://doi.org/https://doi.org/10.1002/wer.1219

Lee, D.-J. (1994). Measurement of bound water in waste activated sludge: Use of the centrifugal settling method. *Journal of Chemical Technology & Biotechnology*, *61*(2), 139-144. https://doi.org/https://doi.org/10.1002/jctb.280610208

Lee, W. S., Chua, A. S. M., Yeoh, H. K., & Ngoh, G. C. (2014). A review of the production and applications of waste-derived volatile fatty acids. *Chemical Engineering Journal*, *235*, 83-99. https://doi.org/https://doi.org/10.1016/j.cej.2013.09.002

Li, X., Peng, Y., Zhao, Y., Zhang, L., & Han, B. (2017). Volatile Fatty Acid Accumulation by Alkaline Control Strategy in Anaerobic Fermentation of Primary Sludge. *Environmental Engineering Science*, *34*(10), 703-710. https://doi.org/10.1089/ees.2016.0399

Li, Y.-Y., & Qiao, W. (2015). Transformations and Impacts of Ammonia and Hydrogen Sulfide in Anaerobic Reactors. In *Anaerobic Biotechnology* (pp. 109-131). https://doi.org/10.1142/9781783267910_0006

Liu, H., Wang, J., Liu, X., Fu, B., Chen, J., & Yu, H.-Q. (2012). Acidogenic fermentation of proteinaceous sewage sludge: Effect of pH. *Water Research*, *46*(3), 799-807. https://doi.org/https://doi.org/10.1016/j.watres.2011.11.047

Liu, N., Jiang, J., Yan, F., Gao, Y., Meng, Y., Aihemaiti, A., & Ju, T. (2018). Enhancement of volatile fatty acid production and biogas yield from food waste following sonication pretreatment. *Journal of Environmental Management*, *217*, 797-804. https://doi.org/https://doi.org/10.1016/j.jenvman.2018.03.135

Liu, Y., Li, X., Kang, X., Yuan, Y., & Du, M. (2014). Short chain fatty acids accumulation and microbial community succession during ultrasonic-pretreated sludge anaerobic fermentation process: Effect of alkaline adjustment. *International Biodeterioration & Biodegradation*, *94*, 128-133. https://doi.org/https://doi.org/10.1016/j.ibiod.2014.07.004

Lizama, A. C., Figueiras, C. C., Herrera, R. R., Pedreguera, A. Z., & Ruiz Espinoza, J. E. (2017). Effects of ultrasonic pretreatment on the solubilization and kinetic study of biogas production from anaerobic digestion of waste activated sludge. *International Biodeterioration & Biodegradation*, *123*, 1-9. https://doi.org/https://doi.org/10.1016/j.ibiod.2017.05.020

Lohani, S. P., & Havukainen, J. (2018). Anaerobic Digestion: Factors Affecting Anaerobic Digestion Process. In S. J. Varjani, E. Gnansounou, B. Gurunathan, D. Pant, & Z. A. Zakaria (Eds.), *Waste Bioremediation* (pp. 343-359). Springer Singapore. https://doi.org/10.1007/978-981-10-7413-4_18

Mailler, R., Gasperi, J., Chebbo, G., & Rocher, V. (2014). Priority and emerging pollutants in sewage sludge and fate during sludge treatment. *Waste Management*, *34*(7), 1217-1226. https://doi.org/https://doi.org/10.1016/j.wasman.2014.03.028

Mao, C., Feng, Y., Wang, X., & Ren, G. (2015). Review on research achievements of biogas from anaerobic digestion. *Renewable and Sustainable Energy Reviews*, *45*, 540-555. https://doi.org/https://doi.org/10.1016/j.rser.2015.02.032

Meegoda, J. N., Li, B., Patel, K., & Wang, L. B. (2018). A Review of the Processes, Parameters, and Optimization of Anaerobic Digestion. *International Journal of Environmental Research and Public Health*, *15*(10), 2224. https://www.mdpi.com/1660-4601/15/10/2224

Mengmeng, C., Hong, C., Qingliang, Z., Shirley, S. N., & Jie, R. (2009). Optimal production of polyhydroxyalkanoates (PHA) in activated sludge fed by volatile fatty acids (VFAs) generated from alkaline excess sludge fermentation. *Bioresource Technology*, *100*(3), 1399-1405. https://doi.org/https://doi.org/10.1016/j.biortech.2008.09.014

Mevik, B.-H., & Wehrens, R. (2007). The pls Package: Principal Component and Partial Least Squares Regression in R. *Journal of Statistical Software*, *18*(2), 1 - 23. https://doi.org/10.18637/jss.v018.i02

Mo, R., Guo, W., Batstone, D., Makinia, J., & Li, Y. (2023). Modifications to the anaerobic digestion model no. 1 (ADM1) for enhanced understanding and application of the anaerobic treatment processes – A comprehensive review. *Water Research*, *244*, 120504. https://doi.org/https://doi.org/10.1016/j.watres.2023.120504

Mohammad Mirsoleimani Azizi, S., Hai, F. I., Lu, W., Al-Mamun, A., & Ranjan Dhar, B. (2021). A review of mechanisms underlying the impacts of (nano)microplastics on anaerobic digestion. *Bioresource Technology*, *329*, 124894. https://doi.org/https://doi.org/10.1016/j.biortech.2021.124894

Murphy, J. D., & Thanasit, T. (2013). 5 - Fundamental science and engineering of the anaerobic digestion process for biogas production. In A. Wellinger, J. Murphy, & D. Baxter (Eds.), *The Biogas Handbook* (pp. 104-130). Woodhead Publishing. https://doi.org/https://doi.org/10.1533/9780857097415.1.104

Negral, L., Marañón, E., Castrillón, L., & Fernández-Nava, Y. (2015). Differences in soluble COD and ammonium when applying ultrasound to primary, secondary and mixed sludge. *Water Science and Technology*, *71*(9), 1398-1406. https://doi.org/10.2166/wst.2015.113

Nges, I. A., & Liu, J. (2010). Effects of solid retention time on anaerobic digestion of dewatered-sewage sludge in mesophilic and thermophilic conditions. *Renewable Energy*, *35*(10), 2200-2206. https://doi.org/https://doi.org/10.1016/j.renene.2010.02.022

Nguyen, V. K., Chaudhary, D. K., Dahal, R. H., Trinh, N. H., Kim, J., Chang, S. W., Hong, Y., La, D. D., Nguyen, X. C., Ngo, H. H., Chung, W. J., & Nguyen, D. D. (2021). Review on pretreatment techniques to improve anaerobic digestion of sewage sludge. *Fuel*, *285*, Article 119105. https://doi.org/10.1016/j.fuel.2020.119105

Nie, E., He, P., Zhang, H., Hao, L., Shao, L., & Lü, F. (2021). How does temperature regulate anaerobic digestion? *Renewable and Sustainable Energy Reviews*, *150*, 111453. https://doi.org/https://doi.org/10.1016/j.rser.2021.111453

Panaro, D. B., Frunzo, L., Mattei, M. R., Luongo, V., & Esposito, G. (2021). Calibration, validation and sensitivity analysis of a surface-based ADM1 model. *Ecological Modelling*, *460*, 109726. https://doi.org/https://doi.org/10.1016/j.ecolmodel.2021.109726

Passos, F., Astals, S., & Ferrer, I. (2014). Anaerobic digestion of microalgal biomass after ultrasound pretreatment. *Waste Management*, *34*(11), 2098-2103. https://doi.org/https://doi.org/10.1016/j.wasman.2014.06.004

Petropoulos, E., Dolfing, J., Davenport, R. J., Bowen, E. J., & Curtis, T. P. (2017). Developing cold-adapted biomass for the anaerobic treatment of domestic wastewater at low temperatures (4, 8 and 15 °C) with inocula from cold environments. *Water Research*, *112*, 100-109. https://doi.org/https://doi.org/10.1016/j.watres.2016.12.009

Pilli, S., Bhunia, P., Yan, S., LeBlanc, R. J., Tyagi, R. D., & Surampalli, R. Y. (2011). Ultrasonic pretreatment of sludge: A review. *Ultrasonics Sonochemistry*, *18*(1), 1-18. https://doi.org/https://doi.org/10.1016/j.ultsonch.2010.02.014

Pilli, S., Yan, S., Tyagi, R. D., & Surampalli, R. Y. (2016). Anaerobic digestion of ultrasonicated sludge at different solids concentrations - Computation of mass-energy balance and greenhouse gas emissions. *Journal of Environmental Management*, *166*, 374-386. https://doi.org/https://doi.org/10.1016/j.jenvman.2015.10.041

Rajagopal, R., Massé, D. I., & Singh, G. (2013). A critical review on inhibition of anaerobic digestion process by excess ammonia. *Bioresource Technology*, *143*, 632-641. https://doi.org/https://doi.org/10.1016/j.biortech.2013.06.030

Ramirez, I., Mottet, A., Carrere, H., Deleris, S., Vedrenne, F., & Steyer, J. P. (2009). Modified ADM1 disintegration/hydrolysis structures for modeling batch thermophilic

anaerobic digestion of thermally pretreated waste activated sludge. *Water Research*, *43*(14), 3479-3492. https://doi.org/10.1016/j.watres.2009.05.023

Refsgaard, J. C., & Storm, B. (1996). Construction, Calibration And Validation of Hydrological Models. In M. B. Abbott & J. C. Refsgaard (Eds.), *Distributed Hydrological Modelling* (pp. 41-54). Springer Netherlands. https://doi.org/10.1007/978-94-009-0257-2_3

Regueira, A., Bevilacqua, R., Mauricio-Iglesias, M., Carballa, M., & Lema, J. M. (2021). Kinetic and stoichiometric model for the computer-aided design of protein fermentation into volatile fatty acids. *Chemical Engineering Journal*, *406*, 126835. https://doi.org/https://doi.org/10.1016/j.cej.2020.126835

Richard, E., Hilonga, A., Machunda, R., & Njau, K. (2019). A review on strategies to optimize metabolic stages of anaerobic digestion of municipal solid wastes towards enhanced resources recovery. *Sustainable Environment Research*, *29*. https://doi.org/10.1186/s42834-019-0037-0

Rosen, C., Vrecko, D., Gernaey, K. V., Pons, M. N., & Jeppsson, U. (2006). Implementing ADM1 for plant-wide benchmark simulations in Matlab/Simulink. *Water Science and Technology*, *54*(4), 11-19. https://doi.org/10.2166/wst.2006.521

Sancho, I., Lopez-Palau, S., Arespacochaga, N., & Cortina, J. L. (2019). New concepts on carbon redirection in wastewater treatment plants: A review. *Science of The Total Environment*, *647*, 1373-1384. https://doi.org/https://doi.org/10.1016/j.scitotenv.2018.08.070

Seiple, T. E., Coleman, A. M., & Skaggs, R. L. (2017). Municipal wastewater sludge as a sustainable bioresource in the United States. *Journal of Environmental Management*, *197*, 673-680. https://doi.org/https://doi.org/10.1016/j.jenvman.2017.04.032

Sharma, K. R. (2008). Kinetics and Modeling in Anaerobic Processes. In *Anaerobic Biotechnology for Bioenergy Production* (pp. 65-92). https://doi.org/https://doi.org/10.1002/9780813804545.ch4

Shi, C., Ma, J., Wu, H., Luo, J., Liu, Y., Li, K., Zhou, Y., & Wang, K. (2022). Evaluation of pH regulation in carbohydrate-type municipal waste anaerobic co-fermentation: Roles

of pH at acidic, neutral and alkaline conditions. *Science of The Total Environment*, *853*, 158327. https://doi.org/https://doi.org/10.1016/j.scitotenv.2022.158327

Shi, X. S., Dong, J. J., Yu, J. H., Yin, H., Hu, S. M., Huang, S. X., & Yuan, X. Z. (2017). Effect of Hydraulic Retention Time on Anaerobic Digestion of Wheat Straw in the Semicontinuous Continuous Stirred-Tank Reactors. *Biomed Res Int*, *2017*, 2457805. https://doi.org/10.1155/2017/2457805

Souza, T. S. O., Ferreira, L. C., Sapkaite, I., Perez-Elvira, S. I., & Fdz-Polanco, F. (2013). Thermal pretreatment and hydraulic retention time in continuous digesters fed with sewage sludge: Assessment using the ADM1. *Bioresource Technology*, *148*, 317-324. https://doi.org/10.1016/j.biortech.2013.08.161

Strazzera, G., Battista, F., Garcia, N. H., Frison, N., & Bolzonella, D. (2018). Volatile fatty acids production from food wastes for biorefinery platforms: A review. *Journal of Environmental Management*, *226*, 278-288. https://doi.org/https://doi.org/10.1016/j.jenvman.2018.08.039

Strong, P. J., McDonald, B., & Gapes, D. J. (2011). Combined thermochemical and fermentative destruction of municipal biosolids: A comparison between thermal hydrolysis and wet oxidative pre-treatment. *Bioresource Technology*, *102*(9), 5520-5527. https://doi.org/https://doi.org/10.1016/j.biortech.2010.12.027

Tchobanoglous, G., Burton, F. L., Stensel, H. D., Metcalf, & Eddy. (2014). *Wastewater engineering : treatment and resource recovery* (5th , revised ed.). McGraw-Hill Higher Education.

Tchounwou, P. B., Yedjou, C. G., Patlolla, A. K., & Sutton, D. J. (2012). Heavy metal toxicity and the environment. *Exp Suppl*, *101*, 133-164. https://doi.org/10.1007/978-3-7643-8340-4_6

Tyagi, V. K., & Lo, S.-L. (2013). Sludge: A waste or renewable source for energy and resources recovery? *Renewable and Sustainable Energy Reviews*, *25*, 708-728. https://doi.org/https://doi.org/10.1016/j.rser.2013.05.029

Valentino, F., Munarin, G., Biasiolo, M., Cavinato, C., Bolzonella, D., & Pavan, P. (2021). Enhancing volatile fatty acids (VFA) production from food waste in a two-phases pilot-

scale anaerobic digestion process. *Journal of Environmental Chemical Engineering*, *9*(5), 106062. https://doi.org/https://doi.org/10.1016/j.jece.2021.106062

Vavilin, V. A., Fernandez, B., Palatsi, J., & Flotats, X. (2008). Hydrolysis kinetics in anaerobic degradation of particulate organic material: An overview. *Waste Management*, *28*(6), 939-951. https://doi.org/https://doi.org/10.1016/j.wasman.2007.03.028

Vavilin, V. A., Rytov, S. V., & Lokshina, L. Y. (1996). A description of hydrolysis kinetics in anaerobic degradation of particulate organic matter. *Bioresource Technology*, *56*(2), 229-237. https://doi.org/https://doi.org/10.1016/0960-8524(96)00034-X

Velghe, F., De Wilde, F., Snellinx, S., Farahbakhsh, S., Belderbos, E., Peral, C., Wiedemann, A., Hiessl, S., Michels, J., Pierrard, M.-A., & Dietrich, T. (2021). Volatile fatty acid platform – a cornerstone for the circular bioeconomy. *FEMS Microbiology Letters*, *368*(9). https://doi.org/10.1093/femsle/fnab056

Vu, C. T. (2017). *Comparison between granular and conventional activated sludge for trace metal elements sorption/desorption. Case of copper for landspreading application in France and in Vietnam*

Comparaison entre des boues d'épuration issues de systèmes conventionnels ou granulaires pour l'adsorption des métaux et l'application au cuivre lors de l'épandage des boues sur des sols Français et Vietnamien (Publication Number 2017LIMO0008) Université de Limoges]. https://theses.hal.science/tel-01661473

Wang, D., Liu, Y., Ngo, H. H., Zhang, C., Yang, Q., Peng, L., He, D., Zeng, G., Li, X., & Ni, B.-J. (2017). Approach of describing dynamic production of volatile fatty acids from sludge alkaline fermentation. *Bioresource Technology*, *238*, 343-351. https://doi.org/https://doi.org/10.1016/j.biortech.2017.04.054

Wichelns, D., Drechsel, P., & Qadir, M. (2015). Wastewater: Economic Asset in an Urbanizing World. *Wastewater: Economic Asset in an Urbanizing World*, 3-14. https://doi.org/10.1007/978-94-017-9545-6_1

Wu, Y., Wang, C., Zheng, M., Zuo, J., Wu, J., Wang, K., & Yang, B. (2017). Effect of pH on ethanol-type acidogenic fermentation of fruit and vegetable waste. *Waste Management*, *60*, 158-163. https://doi.org/https://doi.org/10.1016/j.wasman.2016.09.033

Yesil, H., Molaey, R., Calli, B., & Tugtas, A. E. (2021a). Extent of bioleaching and bioavailability reduction of potentially toxic heavy metals from sewage sludge through pH-controlled fermentation. *Water Research*, *201*, 117303. https://doi.org/https://doi.org/10.1016/j.watres.2021.117303

Yesil, H., Molaey, R., Calli, B., & Tugtas, A. E. (2021b). Removal and recovery of heavy metals from sewage sludge via three-stage integrated process. *Chemosphere*, *280*, 130650. https://doi.org/https://doi.org/10.1016/j.chemosphere.2021.130650

Yeşil, H. (2021). *Selective Separation and Recovery of Heavy Metals from Sewage Sludge Via integrated Anaerobic Bio-Leaching and Membrane Processes* (Publication Number 29442797) [Ph.D., Marmara Universitesi (Turkey)]. ProQuest Dissertations & Theses Global. Turkey. https://www.proquest.com/dissertations-theses/selective-separation-recovery-heavy-metals-sewage/docview/2724662605/se-2?accountid=12251

https://openaccess.marmara.edu.tr/handle/11424/281260

Yu, G.-H., He, P.-J., Shao, L.-M., & He, P.-P. (2008). Toward understanding the mechanism of improving the production of volatile fatty acids from activated sludge at pH 10.0. *Water Research*, *42*(18), 4637-4644. https://doi.org/https://doi.org/10.1016/j.watres.2008.08.018

Yu, L., Wensel, P. C., Ma, J., & Chen, S. (2013). Mathematical modeling in anaerobic digestion (AD). *J Bioremed Biodeg S*, *4*(2).

Zacharof, M.-P., & Lovitt, R. W. (2013). Complex Effluent Streams as a Potential Source of Volatile Fatty Acids. *Waste and Biomass Valorization*, *4*(3), 557-581. https://doi.org/10.1007/s12649-013-9202-6

Zawieja, I. E. (2019). Effect of Thermal and Alkaline Disintegration of Excess Sludge on Biodegradation [journal article]. *Journal of Ecological Engineering*, *20*(10), 172-182. https://doi.org/10.12911/22998993/113151

Zerrouki, S., Rihani, R., Lekikot, K., & Ramdhane, I. (2021). Enhanced biogas production from anaerobic digestion of wastewater from the fruit juice industry by sonolysis: experiments and modelling. *Water Science and Technology*, *84*(3), 644-655. https://doi.org/10.2166/wst.2021.245

Zhang, Q., Hu, J., Lee, D.-J., Chang, Y., & Lee, Y.-J. (2017). Sludge treatment: Current research trends. *Bioresource Technology*, *243*, 1159-1172. https://doi.org/https://doi.org/10.1016/j.biortech.2017.07.070

Zhao, J., Liu, Y., Wang, Y., Lian, Y., Wang, Q., Yang, Q., Wang, D., Xie, G.-J., Zeng, G., Sun, Y., Li, X., & Ni, B.-J. (2018). Clarifying the Role of Free Ammonia in the Production of Short-Chain Fatty Acids from Waste Activated Sludge Anaerobic Fermentation. *ACS Sustainable Chemistry & Engineering*, *6*(11), 14104-14113. https://doi.org/10.1021/acssuschemeng.8b02670

Zhen, G., Lu, X., Kato, H., Zhao, Y., & Li, Y.-Y. (2017). Overview of pretreatment strategies for enhancing sewage sludge disintegration and subsequent anaerobic digestion: Current advances, full-scale application and future perspectives. *Renewable and Sustainable Energy Reviews*, *69*, 559-577. https://doi.org/https://doi.org/10.1016/j.rser.2016.11.187

Zhou, X., Lu, Y., Huang, L., Zhang, Q., Wang, X., & Zhu, J. (2021). Effect of pH on volatile fatty acid production and the microbial community during anaerobic digestion of Chinese cabbage waste. *Bioresource Technology*, *336*, 125338. https://doi.org/https://doi.org/10.1016/j.biortech.2021.125338

Zielińska, M., & Cydzik-Kwiatkowska, A. (2024). Effect of Emerging Micropollutants on the Anaerobic Digestion of Sewage Sludge. *Energies*, *17*(5), 1033. https://www.mdpi.com/1996-1073/17/5/1033

APPENDIX 1

Appendix 1-Table 1. Percentage calculation of VFAs derived from amino acid. Theoretical and determined stoichiometric coefficients was used from Liu et al. (2012)

	Theoretical Stoichiometric Coefficient	Determined Stoichiometric Coefficient	Average Stoichiometric Coefficient	VFA to COD Conversion Factors	Average Stoichiometric Coefficient	
VFAs	**mole/mole AA**	**mole/mole AA**	**mole/mole AA**	**COD/VFA**	**mole COD/ mole AA**	**% Percentage**
Acatic Acid	0.235	0.236	0.2355	1.067	0.2512785	70
Propionic Acid	0.009	0.05	0.0295	1.514	0.044663	12
Butyric Acid	0.025	0.02	0.0225	1.82	0.04095	11
Valeric Acid	0.008	0.015	0.0115	2.04	0.02346	7

Appendix 1-Table 2. Hydrogen included partition percentages of amino acid

Amino Acid Stoichiometric Fractions	% Percentage
Acetic Acid	65
Propionic Acid	11
Butyric Acid	11
Valeric Acid	7
Hydrogen	6

APPENDIX 2

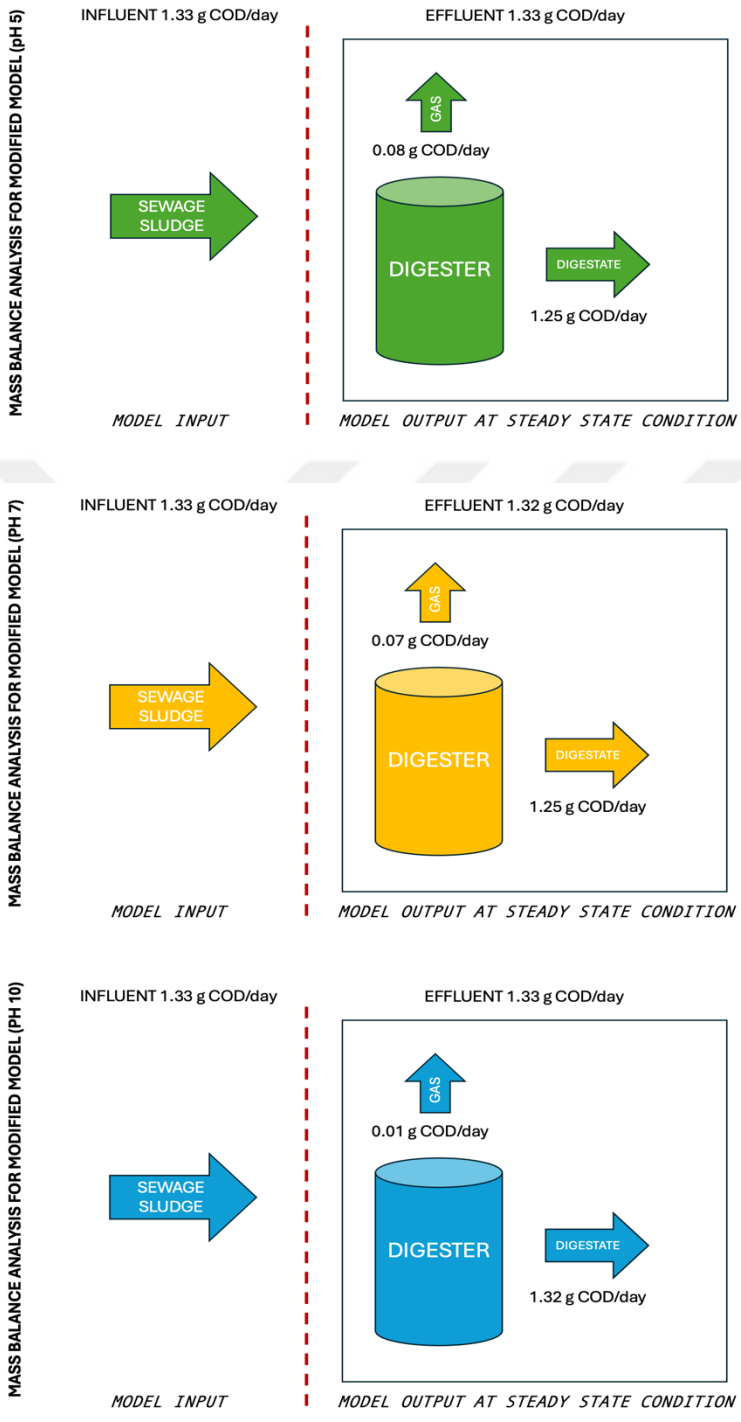

Appendix 2-Figure 1. Mass balance analysis for modified model

APPENDIX 3

```
% --- Initial Parameters of ADM1 --- %

global  Ssu Saa Sfa Sva Sbu Spro Sac Sh2 Sch4 SIC SIN SI...
Xxc Xch Xpr Xli...
Xsu Xaa Xfa Xc4 Xpro Xac Xh2 ...
XI Scat San Shva Shbu Shpro Shac Shco3 Snh3 S_H_ion...
S_gas_h2 S_gas_ch4  S_gas_co2...
f_sI_xc f_xI_xc f_ch_xc f_pr_xc f_li_xc...
N_xc  N_I  N_aa  C_xc C_sI  C_ch C_pr C_li C_xI  C_su  C_aa...
f_fa_li C_fa f_h2_su f_bu_su f_pro_su f_ac_su N_bac C_bu C_pro C_ac C_bac...
Y_su f_h2_aa f_va_aa f_bu_aa f_pro_aa f_ac_aa C_va Y_aa Y_fa Y_c4 Y_pro   C_ch4
Y_ac Y_h2...
K_S_IN k_m_su K_S_su pH_UL_aa pH_LL_aa k_m_aa K_S_aa...
k_m_fa K_S_fa K_Ih2_fa k_m_c4 K_S_c4 K_Ih2_c4 k_m_pro...
K_S_pro K_Ih2_pro k_m_ac K_S_ac pH_UL_ac pH_LL_ac k_m_h2 K_S_h2
pH_UL_h2 pH_LL_h2...
 k_dec_Xsu k_dec_Xaa k_dec_Xfa k_dec_Xc4 k_dec_Xpro k_dec_Xac k_dec_Xh2...
R T_base T_op K_w K_a_va K_a_bu K_a_pro K_a_ac K_a_co2 K_a_IN k_A_Bva
k_A_Bbu k_A_Bpro k_A_Bac...
k_A_Bco2 k_A_BIN kLa K_H_co2 K_H_ch4 K_H_h2...
q_in V_liq  V_gas tres_x ...
P_atm p_gas_h2o q_gas ...
K_I_nh3 FAN ;

f_sI_xc = 0.1;
f_xI_xc = 0.2;
f_ch_xc = 0.2;
f_pr_xc = 0.2;
f_li_xc = 0.3;
Ssu = 0.01;
```

Saa = 0.001;

Sfa = 0.001;

Sva = 0.001;

Sbu = 0.001;

Spro = 0.001;

Sac = 0.001;

Sh2 = 1e-8;

Sch4 = 1e-5;

SIC = 0.04;

SIN = 0.006;

SI = 0;

Xxc = 5.93;

Xch = 0;

Xpr = 0;

Xli = 0;

Xsu = 0.1;

Xaa = 0.1;

Xfa = 0.1;

Xc4 = 0.1;

Xpro = 0.1;

Xac = 0.1;

Xh2 = 0.1;

XI = 0;

Scat = 0.04;

San = 0.02;

Shva = 0;

Shbu = 0;

Shpro = 0;

Shac = 0;

Shco3 = 0;

Snh3 = 0.0055;

FAN = 77.5;

S_H_ion = 1e-10;

S_gas_h2 = 0;

S_gas_ch4 = 0;

S_gas_co2 = 0;

q_gas = 0;

N_xc = 0.0376/14;

N_I = 0.06/14;

N_aa = 0.0077;

C_xc = 0.02786;

C_sI = 0.03;

C_ch = 0.0313;

C_pr = 0.03;

C_li = 0.022;

C_xI = 0.03;

C_su = 0.0313;

C_aa = 0.03;

C_fa = 0.0217;

f_fa_li = 0.95;

f_h2_su = 0.19;

f_bu_su = 0.13;

f_pro_su = 0.27;

f_ac_su = 0.41;

N_bac = 0.08/14;

C_bu = 0.025;

C_pro = 0.0268;

C_ac = 0.0313;

C_bac = 0.0313;

Y_su = 0.1;

f_h2_aa = 0.06;

f_va_aa = 0.07;

f_bu_aa = 0.11;

f_pro_aa = 0.11;

f_ac_aa = 0.65;

C_va = 0.024;

Y_aa = 0.08;

Y_fa = 0.06;

Y_c4 = 0.06;

Y_pro = 0.04;

C_ch4 = 0.0156;

Y_ac = 0.05;

Y_h2 = 0.06;

K_S_IN = 1e-4;

k_m_su = 30;

K_S_su = 0.5;

pH_UL_aa = 8.5;

pH_LL_aa = 4;

k_m_aa = 50;

K_S_aa = 0.3;

k_m_fa = 6;

K_S_fa = 0.4;

K_Ih2_fa = 5e-6;

k_m_c4 = 20;

K_S_c4 = 0.2;

K_Ih2_c4 = 1e-5;

k_m_pro = 13;

K_S_pro = 0.1;

K_Ih2_pro = 3.5e-6;

k_m_ac = 8;

K_S_ac = 0.15;

K_I_nh3 = 0.0018;

pH_UL_ac = 7;

pH_LL_ac = 6;

k_m_h2 = 35;

K_S_h2 = 7e-6;

```
pH_UL_h2 = 6;
pH_LL_h2 = 5;
k_dec_Xsu = 0.02;
k_dec_Xaa = 0.02;
k_dec_Xfa = 0.02;
k_dec_Xc4 = 0.02;
k_dec_Xpro = 0.02;
k_dec_Xac = 0.02;
k_dec_Xh2 = 0.02;
R = 0.083145;
T_base = 273.15;
T_op = T_base + 35;
K_w = 2.08e-14;
K_a_va = 1.38e-5;
K_a_bu = 1.5e-5;
K_a_pro = 1.32e-5;
K_a_ac = 1.74e-5;
K_a_co2 = 4.94e-7;
K_a_IN = 1.11e-9;
k_A_Bva = 1e10;
k_A_Bbu = 1e10;
k_A_Bpro = 1e10;
k_A_Bac = 1e10;
k_A_Bco2 = 1e10;
k_A_BIN = 1e10;
kLa = 200;
q_in = 2e-4;
V_liq = 8e-4;
V_gas = 5e-4;
tres_x = 0;
P_atm = 1.013;
p_gas_h2o = 0.0557;
```

```
K_H_co2 =  0.0271;
K_H_ch4 = 0.00116;
K_H_h2 = 7.38e-4;

time = 0:1:59;

[t,dX]= ode15s('adm1sys',time,[Ssu Saa Sfa Sva Sbu Spro Sac Sh2 Sch4 SIC SIN SI
Xxc Xch Xpr Xli Xsu Xaa Xfa Xc4 Xpro Xac Xh2 XI ...
Scat San Shva Shbu Shpro Shac Shco3 Snh3 S_H_ion S_gas_h2 S_gas_ch4 S_gas_co2
q_gas FAN ]);

filename = 'ADM1BASIC.xlsx';

writematrix(dX,filename,'Sheet',8,'Range','B4:AM63');

% --- MATLAB Implementation of Modified ADM1 for pH10 --- %

function dX=adm1sys(t,X)

global  Ssu Saa Sfa Sva Sbu Spro Sac Sh2 Sch4 SIC SIN SI...
Xxc Xch Xpr Xli Xsu Xaa Xfa  Xc4 Xpro Xac Xh2 ...
XI Scat San Shva Shbu Shpro Shac Shco3 Snh3 S_H_ion...
S_gas_h2 S_gas_ch4  S_gas_co2...
p_gas_h2 p_gas_ch4 p_gas_co2...
rhoT8 rhoT9 rhoT10...
rhoA4 rhoA5 rhoA6 rhoA7 rhoA10 rhoA11 ...
f_sI_xc f_xI_xc f_ch_xc f_pr_xc f_li_xc...
N_xc N_I N_aa C_xc C_sI C_ch C_pr C_li C_xI C_su C_aa...
f_fa_li C_fa f_h2_su f_bu_su f_pro_su f_ac_su N_bac C_bu C_pro C_ac C_bac...
Y_su f_h2_aa f_va_aa f_bu_aa f_pro_aa f_ac_aa C_va Y_aa Y_fa Y_c4 Y_pro C_ch4
Y_ac Y_h2...
k_dis k_hyd_ch k_hyd_pr k_hyd_li K_S_IN k_m_su...
```

```
I_pH_aa I_IN_lim I_pH_ac I_pH_h2 I_h2_fa I_h2_c4 I_h2_pro ...
I5 I6 I7 I8 I9 I10 I11 I12 ...
K_S_su pH_UL_aa pH_LL_aa k_m_aa K_S_aa k_m_fa K_S_fa K_Ih2_fa k_m_c4
K_S_c4 K_Ih2_c4 k_m_pro...
K_S_pro K_Ih2_pro k_m_ac K_S_ac pH_UL_ac k_m_h2 K_S_h2 pH_UL_h2
pH_LL_h2 pH_LL_ac...
k_dec_Xsu k_dec_Xaa k_dec_Xfa k_dec_Xc4 k_dec_Xpro k_dec_Xac k_dec_Xh2...
R T_op K_a_va K_a_bu K_a_pro K_a_ac K_a_co2 K_a_IN k_A_Bva k_A_Bbu
k_A_Bpro k_A_Bac...
k_A_Bco2 k_A_BIN kLa K_H_co2 K_H_ch4 K_H_h2...
q_in V_liq V_gas P_atm p_gas_h2o q_gas ...
FAN pH_op I_nh3 K_I_nh3 ;

if  t<=20
    SIN = 0.006;
    k_dis = 0.7;
    k_hyd_ch = 0.08;
    k_hyd_pr = 0.08;
    k_hyd_li = 0.08;
elseif t>20
    SIN = 0.015;
    k_dis = 0.8;
    k_hyd_ch = 0.8;
    k_hyd_pr = 0.8;
    k_hyd_li = 0.8;
end

dX(33) = S_H_ion - X(33);

pH_op = (-1)*log10(X(33));
```

```
I_pH_aa = (1 + 2*10^(0.5*(pH_LL_aa-pH_UL_aa)))/(1+10^(pH_op -
pH_UL_aa)+10^(pH_LL_aa-pH_op));

I_pH_ac = (1 + 2*10^(0.5*(pH_LL_ac-pH_UL_ac)))/(1+10^(pH_op -
pH_UL_ac)+10^(pH_LL_ac-pH_op));

I_pH_h2 = (1 + 2*10^(0.5*(pH_LL_h2-pH_UL_h2)))/(1+10^(pH_op -
pH_UL_h2)+10^(pH_LL_h2-pH_op));

I_IN_lim = 1 / (1 + K_S_IN / X(11));
I_h2_fa = 1 / (1 + X(8) / K_Ih2_fa);
I_h2_c4 = 1 / (1 + X(8) / K_Ih2_c4);
I_h2_pro = 1 / (1 + X(8) / K_Ih2_pro);
I_nh3 = 1 / (1 + X(32) / K_I_nh3);

I5 = I_pH_aa * I_IN_lim;
I6 = I_pH_aa * I_IN_lim;
I7 = I_pH_aa * I_IN_lim * I_h2_fa;
I8 = I_pH_aa * I_IN_lim * I_h2_c4;
I9 = I_pH_aa * I_IN_lim * I_h2_c4;
I10 = I_pH_aa * I_IN_lim * I_h2_pro;
I11 = I_pH_ac * I_IN_lim * I_nh3;
I12 = I_pH_h2 * I_IN_lim;

rho(1) = k_dis * X(13);
rho(2) = k_hyd_ch * X(14);
rho(3) = k_hyd_pr * X(15);
rho(4) = k_hyd_li * X(16);
rho(5) = k_m_su * (X(1)/(K_S_su + X(1))) * X(17) * I5;
rho(6) = k_m_aa * (X(2)/(K_S_aa + X(2))) * X(18) * I6;
rho(7) = k_m_fa * (X(3)/(K_S_fa + X(3))) * X(19) * I7;
```

```
rho(8) = k_m_c4 * (X(4)/(K_S_c4 + X(4))) * (X(4)/(X(4) + X(5) + 1e-6)) * ((X(20) *
I8));
rho(9) = k_m_c4 * (X(5)/(K_S_c4 + X(5))) * (X(5)/(X(5) + X(4) + 1e-6)) * ((X(20) *
I9));
rho(10) = k_m_pro * (X(6)/(K_S_pro + X(6))) * ((X(21) * I10));
rho(11) = k_m_ac * (X(7)/(K_S_ac + X(7))) * X(22) * I11;
rho(12) = k_m_h2 * (X(8)/(K_S_h2 + X(8))) * X(23) * I12;
rho(13) = k_dec_Xsu * X(17);
rho(14) = k_dec_Xaa * X(18);
rho(15) = k_dec_Xfa * X(19);
rho(16) = k_dec_Xc4 * X(20);
rho(17) = k_dec_Xpro * X(21);
rho(18) = k_dec_Xac * X(22);
rho(19) = k_dec_Xh2 * X(23);

rhoA4 = k_A_Bva * (X(27) * (K_a_va + X(33)) - K_a_va * X(4));
rhoA5 = k_A_Bbu * (X(28) * (K_a_bu + X(33)) - K_a_bu * X(5));
rhoA6 = k_A_Bpro * (X(29) * (K_a_pro + X(33)) - K_a_pro * X(6));
rhoA7 = k_A_Bac * (X(30) * (K_a_ac + X(33)) - K_a_ac * X(7));
rhoA10 = k_A_Bco2 * (X(31) * (K_a_co2 + X(33)) - K_a_co2 * X(10));
rhoA11 = k_A_BIN * (X(32) * (K_a_IN + X(33)) - K_a_IN * X(11));

p_gas_h2 = X(34) * R * T_op/16;
p_gas_ch4 = X(35) * R * T_op/64;
p_gas_co2 = X(36) * R * T_op;

rhoT8 = kLa * (X(8) - 16 * K_H_h2 * p_gas_h2);
rhoT9 = kLa * (X(9) - 64 * K_H_ch4 * p_gas_ch4);
rhoT10 = kLa * (X(10) - X(31) - K_H_co2 * p_gas_co2);

q_gas = ((R * T_op) / (P_atm - p_gas_h2o)) * V_liq * (rhoT8/16 + rhoT9/64 + rhoT10);
q_gas = max(q_gas,0);
```

```
Cvsum1 = (-C_xc + f_sI_xc * C_sI + f_ch_xc * C_ch + f_pr_xc * C_pr + f_li_xc * C_li
+ f_xI_xc * C_xI);
Cvsum2 = (-C_ch + C_su);
Cvsum3 = (-C_pr + C_aa);
Cvsum4 = (-C_li + (1-f_fa_li) * C_su + f_fa_li * C_fa);
Cvsum5 = (-C_su + (1 - Y_su) * (f_bu_su * C_bu + f_pro_su * C_pro + f_ac_su *
C_ac) +Y_su * C_bac);
Cvsum6 = (-C_aa + (1 - Y_aa) * (f_va_aa * C_va + f_bu_aa * C_bu + f_pro_aa *
C_pro + f_ac_aa * C_ac) + Y_aa * C_bac);
Cvsum7 = (-C_fa + (1 - Y_fa) * 0.7 * C_ac + Y_fa * C_bac);
Cvsum8 = (-C_va + (1 - Y_c4) * 0.54 * C_pro + (1 - Y_c4) * 0.31 * C_ac + Y_c4 *
C_bac);
Cvsum9 = (-C_bu + (1 - Y_c4) * 0.8 * C_ac + Y_c4 * C_bac);
Cvsum10 = (-C_pro + (1 - Y_pro) * 0.57 * C_ac + Y_pro * C_bac);
Cvsum11 = (-C_ac + (1 - Y_ac) * C_ch4 + Y_ac * C_bac);
Cvsum12 = ((1 - Y_h2) * C_ch4 + Y_h2 * C_bac);
Cvsum13_19 = (-C_bac + C_xc);

sumproc = Cvsum1 * rho(1) + Cvsum2 * rho(2) + Cvsum3 * rho(3) + Cvsum4 * rho(4)
+...
   Cvsum5 * rho(5) + Cvsum6 * rho(6) + Cvsum7 * rho(7) + Cvsum8 * rho(8) +
Cvsum9 * rho(9) +...
   Cvsum10 * rho(10) + Cvsum11 * rho(11) + Cvsum12 * rho(12)+ Cvsum13_19 *
sum(rho(13:19)) ;

dX(1) = (q_in/V_liq) * (Ssu - X(1)) + rho(2) + (1 - f_fa_li) * rho(4) - rho(5);

dX(2) = (q_in/V_liq) * (Saa - X(2)) + rho(3)  - rho(6);

dX(3) = (q_in/V_liq) * (Sfa - X(3)) + f_fa_li * rho(4) - rho(7);
```

```
dX(4) = (q_in/V_liq) * (Sva - X(4)) + (1 - Y_aa) * f_va_aa * rho(6) - rho(8);

dX(5) = (q_in/V_liq) * (Sbu - X(5)) + (1 - Y_su) * f_bu_su * rho(5) + (1 - Y_aa) *
f_bu_aa * rho(6) - rho(9);

dX(6) = (q_in/V_liq) * (Spro - X(6)) + (1 - Y_su) * f_pro_su * rho(5) + (1 - Y_aa) *
f_pro_aa * rho(6) + (1 - Y_c4) * 0.54 * rho(8) - rho(10);

dX(7) = (q_in/V_liq) * (Sac - X(7)) + (1 - Y_su) * f_ac_su * rho(5) + (1 - Y_aa) *
f_ac_aa * rho(6) + ...
        (1 - Y_fa)* 0.7 * rho(7) + (1 - Y_c4) * 0.31 * rho(8) + (1 - Y_c4) * 0.8 * rho(9)
+ ...
   (1 - Y_pro) * 0.57 * rho(10) - rho(11);

dX(8) = (q_in/V_liq) * (Sh2 - X(8)) + (1 - Y_su) * f_h2_su * rho(5) + (1 - Y_aa) *
f_h2_aa * rho(6) + ...
        (1 - Y_fa) * 0.3 * rho(7) + (1 - Y_c4) * 0.15 * rho(8) + (1 - Y_c4) * 0.2 * rho(9)
+ (1 - Y_pro) * 0.43 * rho(10) - ...
        rho(12) - rhoT8;

dX(9) = (q_in/V_liq) * (Sch4 - X(9)) + (1 - Y_ac) * rho(11) + (1 - Y_h2) * rho(12) -
rhoT9;

dX(10) = (q_in/V_liq) * (SIC - X(10)) - sumproc - rhoT10;

dX(11) = (q_in/V_liq) * (SIN - X(11)) - Y_su * N_bac * rho(5) + (N_aa - Y_aa *
N_bac) * rho(6) - Y_fa * N_bac * rho(7) - ...
        Y_c4 * N_bac * rho(8) - Y_c4 * N_bac * rho(9) - Y_pro * N_bac * rho(10) -
Y_ac * N_bac * rho(11) - ...
        Y_h2 * N_bac * rho(12) + (N_bac - N_xc) * sum(rho(13:19)) + (N_xc - f_xI_xc
* N_I - f_sI_xc * N_I - f_pr_xc * N_aa) * rho(1);
```

```
dX(12) = (q_in/V_liq) * (SI - X(12)) + f_sI_xc * rho(1);

dX(13) = (q_in/V_liq) * (Xxc - X(13)) - rho(1) + sum(rho(13:19));

dX(14) = (q_in/V_liq) * (Xch - X(14)) + f_ch_xc * rho(1) - rho(2);

dX(15) = (q_in/V_liq) * (Xpr - X(15)) + f_pr_xc * rho(1) - rho(3);

dX(16) = (q_in/V_liq) * (Xli - X(16)) + f_li_xc * rho(1) - rho(4);

dX(17) = (q_in/V_liq) * (Xsu - X(17)) + Y_su * rho(5) - rho(13);

dX(18) = (q_in/V_liq) * (Xaa - X(18)) + Y_aa * rho(6) - rho(14);

dX(19) = (q_in/V_liq) * (Xfa - X(19)) + Y_fa * rho(7) - rho(15);

dX(20) = (q_in/V_liq) * (Xc4 - X(20)) + Y_c4 * rho(8) + Y_c4 * rho(9)- rho(16);

dX(21) = (q_in/V_liq) * (Xpro - X(21)) + Y_pro * rho(10)- rho(17);

dX(22) = (q_in/V_liq) * (Xac - X(22)) + Y_ac * rho(11) - rho(18);

dX(23) = (q_in/V_liq) * (Xh2 - X(23)) + Y_h2 * rho(12) - rho(19);

dX(24) = (q_in/V_liq) * (XI - X(24)) + f_xI_xc * rho(1);

dX(25) = (q_in/V_liq) * (Scat - X(25));

dX(26) = (q_in/V_liq) * (San - X(26));

dX(27) = - rhoA4;
```

```
dX(28) = - rhoA5;
dX(29) = - rhoA6;
dX(30) = - rhoA7;
dX(31) = - rhoA10;
dX(32) = - rhoA11;
dX(34) = -((X(34) * q_gas) / V_gas) + rhoT8 * (V_liq/V_gas);
dX(35) = -((X(35) * q_gas) / V_gas) + rhoT9 * (V_liq/V_gas);
dX(36) = -((X(36) * q_gas) / V_gas) + rhoT10 * (V_liq/V_gas);

dX(37) = q_gas - X(37);

FAN = X(32) * 14000 ;

dX(38) = FAN - X(38);

disp([t,SIN,k_hyd_ch,q_gas,S_H_ion,pH_op]);

X0(1) = Ssu;
X0(2) = Saa;
X0(3) = Sfa;
X0(4) = Sva;
X0(5) = Sbu;
X0(6) = Spro;
X0(7) = Sac;
X0(8) = Sh2;
X0(9) = Sch4;
X0(10) = SIC;
X0(11) = SIN;
X0(12) = SI;
X0(13) = Xxc;
X0(14) = Xch;
X0(15) = Xpr;
```

```
X0(16) = Xli;
X0(17) = Xsu;
X0(18) = Xaa;
X0(19) = Xfa;
X0(20) = Xc4;
X0(21) = Xpro;
X0(22) = Xac;
X0(23) = Xh2;
X0(24) = XI;
X0(25) = Scat;
X0(26) = San;
X0(27) = Shva;
X0(28) = Shbu;
X0(29) = Shpro;
X0(30) = Shac;
X0(31) = Shco3;
X0(32) = Snh3;
X0(33) = S_H_ion;
X0(34) = S_gas_h2;
X0(35) = S_gas_ch4;
X0(36) = S_gas_co2;
X0(37) = q_gas;
X0(38) = FAN;

dX=dX(:);
```

CURRICULUM VITAE

Adnan İnan was born in 1988. He completed his primary, secondary, and high school education in İstanbul. In 2012, he graduated from the Environmental Engineering Department, at Bursa Uludağ University. He worked as a Quality Assurance Engineer in the energy transmission, food, and construction sectors. Currently, he is continuing his studies in the Master's Program in Environmental Engineering at Marmara University, which he started in 2021, and he is also running his company, Baupropel İnşaat, established in 2024. In this company, he designs and constructs environmentally friendly buildings with high thermal efficiency, the ability to produce some of their own energy, and low carbon footprints, all while adhering to the principle of sustainability. Outside of his professional life, he writes book reviews, columns, and stories on his website, okuderim.org, which is a product of his interest in reading and writing.